

Image Processing

THOMAS S. HUANG, MEMBER, IEEE, WILLIAM F. SCHREIBER, MEMBER, IEEE, AND OLEH J. TRETIAK, MEMBER, IEEE

Invited Paper

Abstract—Image processing techniques find applications in many areas, chief among which are image enhancement, pattern recognition, and efficient picture coding. Some aspects of image processing are discussed—specifically: the mathematical operations one is likely to encounter, and ways of implementing them by optics and on digital computers; image description; and image quality evaluation. Many old results are reviewed, some new ones presented, and several open questions are posed.

I. INTRODUCTION

IN A BROAD SENSE, the field of image processing deals with the manipulation of data which are inherently two-dimensional in nature. The techniques of image processing find applications in many areas, notably: image enhancement, pictorial pattern recognition, and the efficient coding of pictures for transmission or storage. The common questions underlying these areas are: 1) How do we describe or characterize images? 2) What mathematical operations do we want to use on the images? 3) How do we implement (in hardware) these mathematical operations? 4) How do we evaluate image quality? In the present paper, we shall attempt to discuss some aspects of these questions.

In Sections II and III, we describe some of the more important mathematical operations one encounters in image processing, and in Sections IV, V, and VI the optical and digital computer implementation of these mathematical operations. Then, in Sections VII and VIII, we discuss briefly the problems of image description and image quality evaluation, respectively. Since many excellent review articles on pattern recognition are available [4], [17], [217], [134], [146], [223], and [100], we shall concentrate on image enhancement and efficient picture coding in our paper.

Although most of the techniques we shall describe have been developed and studied by many researchers both at MIT and elsewhere, the way we shall describe them reflects our own personal biases and the experimental results we shall present are mostly our own. Therefore, the reader should be warned at the outset that this is a highly personal paper.

It is impossible, even in this relatively long paper, to cover all the important aspects of image processing. The reader is referred to the Bibliography at the end of the paper for further study. He may also look forward to reading two related special issues of the PROCEEDINGS in 1972, one on digital picture processing and the other on digital pattern recognition.

II. IMAGE ENHANCEMENT

A. The Problem

No imaging system will give images of perfect quality. In image enhancement, we aim to manipulate the image to improve its quality. For example, in aerial reconnaissance (for classifying crops, say)

Manuscript received April 7, 1971; revised August 13, 1971. This work was supported by NIH GMS under Grant 5 P01 GM14940-05. This invited paper is one of a series planned on topics of general interest—The Editor.

The authors are with the Department of Electrical Engineering and Research Laboratory of Electronics, Massachusetts Institute of Technology, Cambridge, Mass. 02139.

and in photographing the planets through the atmosphere, the pictures one gets are degraded by atmospheric turbulence, aberration of the optical system, and relative motion between the camera and the object. In the medical area, a prominent example is radiographs which are usually of low resolution and low contrast. Many electron micrographs are distorted by the spherical aberration of the electron lens. In these and many other similar cases, one would like very much to work on the degraded images to improve their quality.

There are two ways of going about image enhancement. The first way might be called *a priori*. Here, we cleverly design our imaging systems to minimize degradations. Examples of *a priori* methods include the use of sensor and feedback servosystems to compensate for camera motion [25], [46], and [128], and the several unconventional methods of combating atmospherical turbulence—the use of holographic techniques [75], [47], the use of a large optical aperture as a multiple-element interferometer [73], [76], and the ingenious method of Gregory where conventional imaging is used but the camera shutter opens intermittently, exposing the film only when “the seeing is good” [81].

The second way of going about image enhancement might be called *a posteriori*. Here we are given images whose quality needs to be improved. We do not have control over how the image is formed.

Since the variety of *a priori* methods is limited only by the imagination of the inventors, one can hardly make general comments about it—except perhaps saying: “be clever.” Therefore, our discussion in this section will be concentrated on *a posteriori* methods.

We shall approach the problem of *a posteriori* image enhancement from the point of view of image restoration. A general block diagram of the situation is shown in Fig. 1. We shall concern ourselves mainly with two-dimensional monochromatic images. Such an image can be characterized by a real function of two spatial variables, representing the intensity of the image at a spatial point. We assume that an ideal image $f(x, y)$ would be obtained if our imaging system were perfect. But since our imaging system is not perfect, we get a degraded image $g(x, y)$. The purpose of image restoration is to work on the degraded image to get an improved image $\hat{f}(x, y)$ which is as close to the ideal image $f(x, y)$ as possible according to, e.g., the mean-square error criterion.

B. A Special Class of Degrading Systems

In general, the degrading system could be very complex. However, in many cases of practical importance, such as camera motion, atmospheric turbulence, and blurring due to the optical transfer functions of lenses, the degrading systems can be modeled by the block diagram shown in Fig. 2. The ideal image $f(x, y)$ is first acted on by a linear system with impulse response $k(x, y; \alpha, \beta)$:

$$g_1(x, y) = \int \int_{-\infty}^{\infty} k(x, y; \alpha, \beta) f(\alpha, \beta) d\alpha d\beta. \quad (1)$$

Then g_1 goes through a nonlinear amnesic (memoryless) system with a transfer characteristic $T(\cdot)$. The output of an amnesic system at any particular spatial point depends only on the corresponding

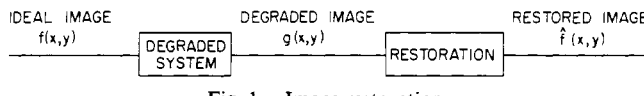


Fig. 1. Image restoration.

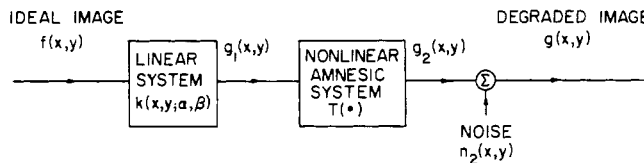


Fig. 2. A special class of degrading systems.

point of the input but no other points. Therefore,

$$g_2(x_0, y_0) = T(g_1(x_0, y_0)) \quad (2)$$

where (x_0, y_0) is any given spatial point. Finally, a noise $n_2(x, y)$ is added to g_2 to yield the degraded image:

$$g(x, y) = g_2(x, y) + n_2(x, y). \quad (3)$$

The nonlinearity and the noise are usually due to the detector (such as film) in the imaging system.

In some cases, the linear system in Fig. 2 is shift-invariant

$$k(x, y; \alpha, \beta) = h(x - \alpha, y - \beta). \quad (4)$$

Then the superposition integral (1) can be written as a convolution

$$g_1(x, y) = \int \int_{-\infty}^{\infty} h(x - \alpha, y - \beta) f(\alpha, \beta) d\alpha d\beta = h \otimes f. \quad (5)$$

A linear system that is not shift-invariant will be called shift-varying.

C. Restoring Images Degraded by Linear Shift-Invariant (LSI) Systems

1) *The Fourier Transform Approach:* Let us assume that we know the transfer characteristic T of our detector and let us assume for the time being that the noise n_2 is negligible. Then by applying T^{-1} , the inverse of T , to the degraded image, we will obtain g_1 (cf., Fig. 2). The remaining task is to recover the ideal image f from g_1 . This can be done easily, if the linear system is shift-invariant (LSI), because from (5) we have

$$F(u, v) = \frac{G_1(u, v)}{H(u, v)} \quad (6)$$

where F , G_1 , and H are the two-dimensional Fourier transforms of f , g_1 , and h , respectively, and u and v are spatial frequencies.

2) *Noise:* In reality, of course, noise is always present. Therefore, after applying T^{-1} to the degraded image g (cf., Fig. 2) we will get

$$p(x, y) = g_1(x, y) + n_1(x, y) = f \otimes h + n_1 \quad (7)$$

where $n_1(x, y)$ is noise. We can still try to estimate $F(u, v)$ by

$$\hat{F}(u, v) = \frac{P(u, v)}{H(u, v)} \quad (8)$$

where P is the Fourier transform of p . However, we will get into trouble where $H(u, v)=0$. One way to remedy this is to modify the right-hand side of (8), replacing $1/H$ by zero in the range of (u, v) over which the noise is larger than the signal [91].

Alternatively, we can find an optimum linear shift-invariant filter which, when acting upon the noisy degraded image $p(x, y)$, will

give an estimation of the ideal image f with the least mean-square error. It can be shown [97] that, when f and n_1 are statistically uncorrelated, such an optimum filter has the frequency response

$$Q(u, v) = \frac{H^*(u, v)\Phi_f(u, v)}{|H(u, v)|^2\Phi_f(u, v) + \Phi_n(u, v)} \quad (9)$$

where Φ_f and Φ_n are the power density spectra of the ideal image f and the noise n_1 , respectively, and $*$ denotes complex conjugation. And the minimum mean-square error is

$$E_{\min} = \int \int_{-\infty}^{\infty} \frac{\Phi_f(u, v)\Phi_n(u, v)}{|H(u, v)|^2\Phi_f(u, v) + \Phi_n(u, v)} du dv. \quad (10)$$

Note that when $n_1=0$, $Q=1/H$, which is the simple inverse filter used in (8). Slepian [202] also solved the least mean-square estimation problem for the case where the degrading impulse response h is stochastic. The optimum filter was found to be again given by (9), except that H^* and $|H|^2$ are replaced by \bar{H}^* and $\bar{|H|^2}$, where the overbars denote ensemble averages.

Experiments with laboratory-simulated degraded imagery indicated that [103], [104] the optimum filter (9) gave much better recovered images than the simple inverse filter used in (8). However, the case of finding good restoration filters is by no means closed. First of all, detector noise is not uncorrelated with the ideal image [164], [106], [61]. Secondly, the filter (9) is optimum only among all linear shift-invariant filters. There certainly may be linear shift-varying and nonlinear filters which perform much better. In searching for good filters for signal-dependent noise, one promising approach seems to be the use of adaptive filters [52a], [170].

3) *Restoration Beyond the Diffraction Limit:* Even in the absence of noise, the estimation (8) gets into trouble when $H(u, v)$ is zero outside a certain range of (u, v) .

In the presence of noise, our optimum LSI filter $Q(u, v)$ is given by (9). Note that $Q(u, v)=0$ wherever $H(u, v)=0$. Therefore, by using Q , we cannot hope to recover $F(u, v)$ outside the range of (u, v) where $H(u, v)$ is nonzero.

In reality, all optical imaging systems are limited by diffraction. Therefore, the degrading frequency response $H(u, v)$ will be zero for $(u^2 + v^2) \geq A$ where A is a constant. Is there any hope of restoring image detail beyond the diffraction limit? The answer is a qualified yes. There is a way out if the ideal image $f(x, y)$ is of finite extent; because then $F(u, v)$ is analytic, and once we have determined $F(u, v)$ within a certain range of (u, v) , we can use analytic continuation to extend our solution to all (u, v) . Harris [90] discussed several practical methods of carrying out the analytic continuation. On a theoretical basis, the method of analytic continuation proposed by Slepian [204] is perhaps most satisfying. It makes use of prolate spheroidal wave functions. We note that the operation of analytic continuation is linear but shift-varying.

The presence of noise introduces severe errors in analytic continuation [228], [48], [66]. In one example [93] it was found that in order to succeed in analytic continuation a noise to signal amplitude ratio of around 1:1000 was required.

4) *Analytic Continuation Using Prolate Spheroidal Wave Functions (PSWF):* We now describe briefly the procedure of doing analytic continuation using PSWF. We first review the properties of PSWF [212], [63], [204], [138], [139], [200], [201], [205] following Slepian and Pollak.

Given $T > 0$ and any $\Omega > 0$, we can find a countably infinite set of real functions $\{\psi_i(t); i=0, 1, 2, \dots\}$ and a set of real positive numbers $\lambda_0 > \lambda_1 > \lambda_2 > \dots$ such that:

1) $\Psi_i(\omega)$, the Fourier transform of $\psi_i(t)$, vanishes for $|\omega| > \Omega$, and $\psi_i(t)$ are orthonormal on the real line, and complete in the class of

functions whose Fourier transform vanishes for $|\omega| > \Omega$

$$\int_{-\infty}^{\infty} \psi_i(t) \psi_j(t) dt = \begin{cases} 0, & i \neq j \\ 1, & i = j \end{cases} \quad i, j = 0, 1, 2, \dots \quad (11)$$

2) In the interval $-T/2 \leq t \leq T/2$, $\psi_i(t)$ are orthogonal and complete in the class of all square integrable functions:

$$\int_{-T/2}^{T/2} \psi_i(t) \psi_j(t) dt = \begin{cases} 0, & i \neq j \\ \lambda_i, & i = j \end{cases} \quad i, j = 0, 1, 2, \dots \quad (12)$$

a) $\sum_{n=0}^{\infty} \frac{1}{\lambda_n} \psi_n(t) \psi_n(t') = \delta(t - t')$ (13)

where $\delta(t)$ is the unit impulse function.

3) For all values of t , real or complex

$$\lambda_i \psi_i(t) = \int_{-T/2}^{T/2} \frac{\sin \Omega(t-S)}{\pi(t-S)} \psi_i(S) dS, \quad i = 0, 1, 2, \dots \quad (14)$$

a) $K_n \psi_n(t) = \frac{1}{2\pi} \int_{-\Omega}^{\Omega} e^{j\omega t} \psi_n\left(\frac{\omega T}{2\Omega}\right) d\omega \quad (15)$

where K_n is a constant depending on n .

4) Both $\psi_i(t)$ and λ_i are functions of $C \equiv \Omega T/2$. Note that the number of independent samples in the interval $-T/2 \leq t \leq T/2$ for a function bandlimited to $(-\Omega, \Omega)$ is $(2/\pi)C$. For a fixed value of C , the λ_i fall off to zero rapidly with increasing i once i has exceeded $(2/\pi)C$.

$$5) \quad \psi_n(-t) = (-1)^n \psi_n(t). \quad (16)$$

We now come back to our problem of analytic continuation. We assume that a real function $f(x, y)$ satisfies

$$f(x, y) = 0, \quad \text{for } |x| > A \quad \text{or} \quad |y| > B \quad (17)$$

where A and B are constants. We know the value of $F(u, v)$, the Fourier transform of $f(x, y)$, in $|u| \leq \alpha/2$ and $|v| \leq \beta/2$ where α and β are constants. We want to determine the value of $F(u, v)$ for all u and v . We proceed as follows. Let $\{\psi_i(u); \lambda_i\}$ be the set of PSWF and their corresponding eigenvalues with $T = \alpha$ and $\Omega = A$, and let $\{\phi_j(v); \mu_j\}$ be those with $T = \beta$ and $\Omega = B$. Then from property 1) we can expand $F(u, v)$ in terms of ψ_i and ϕ_j

$$F(u, v) = \sum_{i=0}^{\infty} \sum_{j=0}^{\infty} a_{ij} \psi_i(u) \phi_j(v), \quad \text{for all } u \text{ and } v. \quad (18)$$

Multiplying both sides of (18) by $\psi_m(u) \phi_n(v)$ and integrating from $u = -\alpha/2$ to $\alpha/2$ and $v = -\beta/2$ to $\beta/2$, and using (12), we get

$$a_{mn} = \frac{1}{\lambda_m \mu_n} \int_{u=-\alpha/2}^{\alpha/2} \int_{v=-\beta/2}^{\beta/2} F(u, v) \psi_m(u) \phi_n(v) du dv. \quad (19)$$

Since we know $F(u, v)$ in $|u| \leq \alpha/2$ and $|v| \leq \beta/2$, we can calculate a_{ij} ($i, j = 0, 1, 2, \dots$) from (19). Then, substituting the values of a_{ij} into (18), we get $F(u, v)$ for all u and v .

We note that the function $F(u, v)$ is in general complex. However, it is easily shown that both its real and imaginary parts have inverse Fourier transforms that vanish for $|x| > A$ or $|y| > B$. Therefore, (18) is valid with complex coefficients a_{ij} . In fact, since $f(x, y)$ is limited in extent, the real and imaginary parts of $F(u, v)$ are related by the Hilbert transform [84]; so it is necessary to work only with the real or imaginary part.

In practical calculations, (18) has to be truncated:

$$F_{MN}(u, v) = \sum_{i=0}^{M-1} \sum_{j=0}^{N-1} a_{ij} \psi_i(u) \phi_j(v), \quad \text{for all } u \text{ and } v. \quad (20)$$

The mean-square error due to this truncation is

$$\int \int_{-\infty}^{\infty} |F(u, v) - F_{MN}(u, v)|^2 du dv = \sum_{i=M}^{\infty} \sum_{j=N}^{\infty} |a_{ij}|^2. \quad (21)$$

Also, in practice, we always have noise. Instead of knowing $F(u, v)$ we know only

$$F_C(u, v) = F(u, v) + N(u, v) \quad (22)$$

where $N(u, v)$ is noise. Using F_C instead of F in the integral of (19), we get instead of (18):

$$F_C(u, v) = \sum_{i=0}^{\infty} \sum_{j=0}^{\infty} a'_{ij} \psi_i(u) \phi_j(v), \quad \text{for all } u \text{ and } v \quad (23a)$$

where

$$a'_{ij} = a_{ij} + n_{ij} \quad (23b)$$

and

$$n_{ij} = \frac{1}{\lambda_i \mu_j} \int_{u=-\alpha/2}^{\alpha/2} \int_{v=-\beta/2}^{\beta/2} N(u, v) \psi_i(u) \phi_j(v) du dv. \quad (24)$$

After truncation, we have

$$F_{C,MN}(u, v) = \sum_{i=0}^{M-1} \sum_{j=0}^{N-1} (a'_{ij}) \psi_i(u) \phi_j(v), \quad \text{for all } u \text{ and } v. \quad (25)$$

Therefore, in practice, what we get is $F_{C,MN}(u, v)$. The question is how close is $F_{C,MN}$ to the desired F over all u and v ?

The error between $F_{C,MN}$ and F is

$$\begin{aligned} \epsilon(u, v) \equiv F - F_{C,MN} &= \sum_{i=M}^{\infty} \sum_{j=N}^{\infty} a_{ij} \psi_i(u) \phi_j(v) \\ &\quad - \sum_{i=0}^{M-1} \sum_{j=0}^{N-1} n_{ij} \psi_i(u) \phi_j(v). \end{aligned} \quad (26)$$

The first term at the right-hand side of (26) is the error due to truncation, while the second term is the error due to noise. We denote the second term by

$$N_{MN}(u, v) \equiv \sum_{i=0}^{M-1} \sum_{j=0}^{N-1} n_{ij} \psi_i(u) \phi_j(v), \quad \text{for all } u \text{ and } v. \quad (27)$$

Then assuming the noise $N(u, v)$ has zero mean and is white, i.e.,

$$\overline{N(u, v)} = 0 \quad (28)$$

$$\overline{N(u_1, v_1) N(u_2, v_2)} = K \delta(u_1 - u_2, v_1 - v_2) \quad (29)$$

where K is a constant and the superbars denote ensemble averages, we get

$$\overline{N_{MN}(u, v)} = 0 \quad (30)$$

$$\overline{N_{MN}^2(u, v)} = K \sum_{i=0}^{M-1} \sum_{j=0}^{N-1} \frac{1}{\lambda_i \mu_j} \psi_i^2(u) \phi_j^2(v), \quad \text{for all } u \text{ and } v \quad (31)$$

and

$$\int \int_{-\infty}^{\infty} \overline{\epsilon^2(u, v)} du dv = \sum_{i=M}^{\infty} \sum_{j=N}^{\infty} |a_{ij}|^2 + K \sum_{i=0}^{M-1} \sum_{j=0}^{N-1} \frac{1}{\lambda_i \mu_j}. \quad (32)$$

Remembering that λ_i and μ_j decrease with increasing i and j , we see from (32) that while the truncation error decreases with increasing M and N , the error due to noise increases with increasing M and N . Although we have not done any detailed noise analysis, the situation

does not seem promising. On the one hand, since the number of independent samples of $F(u, v)$ in $|u| \leq \alpha/2$ and $|v| \leq \beta/2$ is $(A\alpha/\pi)(B\beta/\pi)$, we do not expect to be able to make the truncation error small unless $M \gg A\alpha/\pi$ and $N \gg B\beta/\pi$. On the other hand, when $i > A\alpha/\pi$ and $j > B\beta/\pi$, λ_i and μ_j will decrease rapidly with increasing i and j (property 4), so that the error due to noise will be large.

A more satisfying way to resolve this truncation versus noise problem is as follows. Instead of using a'_{ij} as an estimation for a_{ij} as we did in (23a), we use the least mean-square linear estimation

$$\hat{a}_{ij} = a'_{ij} \left(1 + \frac{n_{ij}^2}{a_{ij}^2} \right)^{-1} \quad (33)$$

Then, when i and j are such that the noise power is much greater than the signal power, \hat{a}_{ij} becomes very small, which essentially truncates the infinite series in (23a).

5) Integral Equation Approach: Alternatively, we can solve the problem discussed in the preceding section in the spatial domain via the solution of an integral equation [34], [181], [216]. Let

$$F_T(u, v) = F(u, v)W(u, v) \quad (34)$$

where

$$W(u, v) = \begin{cases} 1, & \text{for } |u| \leq \frac{\alpha}{2}, \text{ and } |v| \leq \frac{\beta}{2} \\ 0, & \text{elsewhere.} \end{cases} \quad (35)$$

The problem is: Given $F_T(u, v)$, find $F(u, v)$ for all u and v . Taking the inverse Fourier transform of both sides of (34), we get

$$f_T(x, y) = f(x, y) \otimes w(x, y) \\ = \int_{\zeta=-A}^A \int_{\eta=-B}^B f(\zeta, \eta) w(x - \zeta, y - \eta) d\zeta d\eta \quad (36)$$

where f_T , f , and w are the inverse Fourier transforms of F_T , F , and W , respectively, and as before, we assume $f(x, y) = 0$ for $|x| > A$ or $|y| > B$. The inverse Fourier transform of $W(u, v)$ is

$$w(x, y) = \frac{\sin(x\alpha/2)}{\pi x} \cdot \frac{\sin(y\beta/2)}{\pi y}. \quad (37)$$

In the spatial domain, our problem becomes: Given $f_T(x, y)$, find $f(x, y)$. That is, we want to solve the integral equation (36).

From property 3) of the preceding section, we know that the eigenfunctions and eigenvalues for the kernel $w(x, y)$ are $\{\Psi_i(x)\Phi_j(y); i, j = 0, 1, 2, \dots\}$, where $\{\Psi_i(x); \lambda'_i\}$ are PSWF with $\Omega = \alpha/2$ and $T = 2A$, and $\{\Phi_j(y); \mu'_j\}$ those with $\Omega = \beta/2$ and $T = 2B$. Expanding $f(x, y)$ in terms of the eigenfunctions

$$f(x, y) = \sum_{i=0}^{\infty} \sum_{j=0}^{\infty} b_{ij} \Psi_i(x) \Phi_j(y), \quad \text{for } |x| \leq A \text{ and } |y| \leq B. \quad (38)$$

Substituting in (36) and using (14),

$$f_T(x, y) = \sum_{i=0}^{\infty} \sum_{j=0}^{\infty} b_{ij} \lambda'_i \mu'_j \Psi_i(x) \Phi_j(y), \quad \text{for } |x| \leq A \text{ and } |y| \leq B. \quad (39)$$

Multiplying both sides by $\Psi_m(x)\Phi_n(y)$ and integrating from $x = -A$ to A and from $y = -B$ to B , we get

$$b_{mn} = \frac{1}{\lambda'_m \mu'_n} \int_{x=-A}^A \int_{y=-B}^B f_T(x, y) \Psi_m(x) \Phi_n(y) dx dy. \quad (40)$$

To summarize, the procedure is to first calculate b_{mn} from (40) and then substitute them into (38) to get $f(x, y)$. Of course, in practice, we again have errors due to truncation and noise.

6) Boundary Conditions: In deriving the optimum filter $Q(u, v)$ given in (9), it was assumed tacitly that we had the degraded image $p(x, y)$ of (7) available for all (x, y) . In reality, we will have only a finite piece of it. For example, we may know $p(x, y)$ only in the region $R = \{|x| \leq A/2 \text{ and } |y| \leq B/2\}$, where A and B are constants. Let

$$p_r(x, y) = \begin{cases} p(x, y), & \text{in } R = \left\{ |x| \leq \frac{A}{2} \text{ and } |y| \leq \frac{B}{2} \right\} \\ 0, & \text{elsewhere.} \end{cases} \quad (41)$$

Then what we can do is to apply our optimum inverse filter to p_r to get $p_r(x, y) \otimes q(x, y)$, where $q(x, y)$ is the inverse Fourier transform of $Q(u, v)$. Under what conditions will $p_r \otimes q$ equal $p \otimes q$ which is our desired result? They will be equal if the original image $f(x, y)$ consists of a small object lying in a uniform background (assuming that the object lies in R). If the original image $f(x, y)$ is not uniform outside R , things will still be all right if the extent of $q(x, y)$ is small compared with the size of R , i.e., if

$$q(x, y) \approx 0, \quad \text{for } (x^2 + y^2) \geq D$$

where D is a constant, and $D \ll A, B$.

Then

$$p_r \otimes q \approx p \otimes q, \quad \text{for } |x| \leq \frac{A-D}{2} \text{ and } |y| \leq \frac{B-D}{2}.$$

What can we do if the original image $f(x, y)$ is not uniform outside the region R and if the extent of $q(x, y)$, the impulse response of the inverse filter, is not small compared to the size of R ? The answer is that under certain conditions, we do have a way out via analytic continuation. If either the original image $f(x, y)$ or the impulse response $h(x, y)$ of the degrading system is bandlimited, i.e., if either $F(u, v)$ or $H(u, v)$ is zero for $(u^2 + v^2) \geq K$ where K is a constant, then $f \otimes h$ will be an analytic function. Neglecting the noise n_1 in (7), we can say that $p(x, y)$ is analytic. Therefore, we can use analytic continuation to extend $p_r(x, y)$ to outside of R and thereby obtain $p(x, y)$ for all (x, y) . Then we can apply the optimum inverse filter q to $p(x, y)$. In this way, we can recover $f(x, y)$ not only in R but in fact for all (x, y) [175], [176]. Again, the inevitable noise will be the limiting factor of this procedure.

7) Linear Motion Degradation: In the preceding sections, we discussed in general terms the restoration of images degraded by LSI systems. For any particular type of degradation, special methods may be available. A case in point is linear motion-degraded images, which were studied by various researchers [203], [92], [214].

8) Other Approaches: In the preceding sections we have discussed the Fourier transform approach of solving the integral equation (7). Several other approaches are worth noting.

Jansson [121], [120], [122], proposed an iterative method of solving (7), which can best be implemented digitally. A similar approach was used by Shaw [197]. In a method due to MacAdam [151], the digitized version of (7) was first transformed into a one-dimensional form, and then the inverse filtering or deconvolution was done by essentially dividing the Z transform (in polynomial form) corresponding to p by that corresponding to h . MacAdam developed an algorithm which could do the deconvolution with the constraint that the values of the samples of p , f , and h lie in prescribed ranges. The major disadvantage of these methods is that when the image to be restored contains a large number of resolvable points, the computation time may become unreasonably long.

It is interesting to mention the alternative formulation of the restoration problem by Smith [207]. He studied the problem of determining LSI filter $r(x, y)$ which would minimize the "width" of $r \otimes h$ (where h is the degrading filter) under the condition that the

signal-to-noise ratio in $p \otimes h \otimes r$ is kept constant. In general, no closed-form solution can be found. However, Smith's numerical example indicates that the filter $r(x, y)$ has the same characteristics as the optimum inverse filter $q(x, y)$ of (9).

9) Multiframe Processing: In some applications, we have available to us several pictures of the same object degraded by different LSI systems. This is the case, e.g., when we take a sequence of short-exposure pictures of a relatively stationary object through a turbulent medium such as the atmosphere. Let us assume that the exposure time of each picture is short so that the turbulent medium is "frozen" for each frame, and let us assume that the object remains unchanged during our picture taking. Then the degraded images will be (if we neglect detector noise)

$$p_i(x, y) = f(x, y) \otimes h_i(x, y), \quad i = 1, 2, \dots, M \quad (42)$$

where $f(x, y)$ is the ideal image, and $h_i(x, y)$ the impulse response of the turbulent medium at the instant of time when the i th picture was taken. It should be mentioned here that generally a turbulent medium can be modeled better by a linear shift-varying (LSV) system. However, under certain conditions (e.g., when the turbulent medium is very close to the entrance pupil of the camera and very far away from the object, and the object is small—this is the case when we take telescopic pictures of a planet or an artificial satellite from the earth), the LSI model is a reasonable approximation.

The impulse responses $h_i(x, y)$ are random in nature and can be considered as noise in (42). This noise, rather than added to the signal f , is convolved with it. However, we can change the situation to the more familiar additive one, by taking the Fourier transform of both sides of (42) and then taking the logarithm [165]. We get

$$\log P_i(u, v) = \log F(u, v) + \log H_i(u, v), \quad i = 1, 2, \dots, M \quad (43)$$

where P_i , F , and H_i are the Fourier transforms of p_i , f , and h_i , respectively.

Now we can apply to (43) any techniques of statistical estimation which are appropriate for additive noise. In particular, we can sum both sides of (43) over i ,

$$\sum_{i=1}^M \log P_i(u, v) = M \log F(u, v) + \sum_{i=1}^M \log H_i(u, v). \quad (44)$$

We expect that the summation at the right-hand side of (44) is almost a constant (K , say) for a reasonably large M . Therefore,

$$F(u, v) \simeq \left[\prod_{i=1}^M P_i(u, v) \right]^{1/M} e^{-K/M}. \quad (45)$$

Therefore, except for a multiplicative constant, we can estimate $F(u, v)$ by

$$\hat{F}(u, v) = \left[\prod_{i=1}^M P_i(u, v) \right]^{1/M} \quad (46)$$

or

$$|\hat{F}(u, v)| = \left[\prod_{i=1}^M |P_i(u, v)| \right]^{1/M} \quad (47a)$$

and

$$\angle \hat{F}(u, v) = \frac{1}{M} \sum_{i=1}^M \angle P_i(u, v) \quad (47b)$$

where we have used $\angle Z$ to denote the phase angle of the complex number Z .

In a slightly different approach, Harris [89] argued that atmo-

spheric turbulence could only decrease the magnitude of each spatial frequency component of the object. Therefore, for each pair of values $u = u_0$ and $v = v_0$, he used the estimation

$$|\hat{F}(u_0, v_0)| = \max_i |P_i(u_0, v_0)|. \quad (48)$$

For the phase angle, (47b) was used. Laboratory simulation indicated that Harris' method worked quite well.

A more elaborate discussion on statistical estimation was given by Kennedy [131]. Also Moldon [159] suggested a method of estimating $F(u, v)$ by taking a large number of independent measurements of the short-term mutual coherence function at the entrance pupil of the imaging system and then averaging the results appropriately.

D. Determining the Characteristics of LSI Degrading Systems

In Section II-C, we discussed the restoration of images degraded by LSI systems, assuming that we know the impulse response $h(x, y)$ of the degrading system. We now ask the question: How do we determine $h(x, y)$? Some comments on terminology are in order. The impulse response $h(x, y)$ of an optical system is usually referred to as its point spread function (PSF); the Fourier transform $H(u, v)$ its optical transfer function (OTF). The magnitude of the OTF is called the modulation transfer function (MTF). The response of an optical system to a sharp line (i.e., an impulse sheet) is called its line spread function (LSF). When the system is linear shift-varying (LSV), the PSF still makes sense, but the OTF does not. The shape of the PSF of an LSV system will, of course, vary with the position of the input point.

1) Measurement of Degrading System: In some cases, the degrading system is available to us. For example, we may have the camera-film system which we used to get our pictures. Then, we can simply measure either the PSF or the OTF of the lens and film [68], [227], [209]. It should be mentioned that some of the degrading effects of lens and film are LSV and nonlinear. However, if we have the degrading system available to us, we can try to measure the LSV and nonlinear characteristics as well. One prominent example was the work carried out at the Jet Propulsion Laboratory in connection with the Ranger and Mariner pictures of the moon and Mars [161]. Extensive measurements were made on the vidicon camera system before the satellite was launched. Later, the received pictures were enhanced superbly using these measured characteristics.

In many other cases, however, either the degrading system is not available to us or it is time-varying (e.g., atmospheric turbulence). Then we have to think of other ways of estimating its characteristics.

2) Theoretical Analysis: By postulating a reasonable model for an LSI degrading system, we can often calculate theoretically its PSF or OTF. For example, a defocused lens, from a geometrical-optics point of view, can be thought of as having a PSF which is constant and nonzero in a circular disk and zero elsewhere. A more accurate calculation would involve the effect of diffraction [73], [74]. It can be shown that [101], [102], [211] when the defocusing is large, the geometrical OTF agrees well with the diffraction OTF for low spatial frequencies.

The PSF due to lens aberration can also be calculated theoretically [158], [42], [33], [177]. However, except for spherical aberrations (which can be approximated by an LSI system) the other aberrations are definitely LSV. For third-order spherical aberration, the PSF is approximately

$$h(x, y) = \begin{cases} \frac{1}{12\pi B^{2/3} d^2} (x^2 + y^2)^{-2/3}, & \text{for } \sqrt{x^2 + y^2} \leq BR^3 \\ 0, & \text{for } \sqrt{x^2 + y^2} > BR^3 \end{cases} \quad (49)$$

where d is the distance between the object and the exit pupil, R the

radius of the exit pupil, and B the spherical aberration coefficient. We have adopted the convention here that the spatial coordinates in the image plane are scaled by a factor M (the lateral magnification) so that the imaging system can be considered as an LSI system.

The calculation of the PSF due to a relative translational motion between the object and the camera during exposure has been done by many researchers [177], [190], [166], [207b]. Let the motion be described by

$$\begin{aligned} x &= a(t) \\ y &= b(t) \end{aligned} \quad (50)$$

where $a(t)$ and $b(t)$ are functions of the time variable t . Then the PSF is

$$h(x, y) = \int_{-T/2}^{+T/2} \delta(x - a(t), y - b(t)) dt \quad (51a)$$

where we have assumed $(-T/2, T/2)$ to be the exposure time interval. The corresponding OTF is

$$H(u, v) = \int_{-T/2}^{T/2} \exp(-j[u a(t) + v b(t)]) dt. \quad (51b)$$

For example, if the motion is linear and uniform (along the x direction, say)

$$\begin{aligned} x &= kt \\ y &= 0 \end{aligned} \quad (52)$$

where k is a constant, we have

$$H(u, v) = T \frac{\sin(kuT/2)}{kuT/2}. \quad (53)$$

If the motion is simple harmonic (along the x direction, say) with a period equal to T ,

$$\begin{aligned} x &= A \cos \frac{2\pi}{T} t \\ y &= 0 \end{aligned} \quad (54)$$

where A is a constant, the OTF is

$$H(u, v) = J_0(Au) \quad (55)$$

where J_0 is the Bessel function of the zeroth order.

Several researchers have considered the effects on motion OTF by camera shutter operation [167], [98], [191] and by the exponentially-decaying response of some detectors [145].

The OTF due to atmospheric turbulence was calculated by Hufnagel and Stanley, and Fried [117], [116], [64], [65], [150]. For long exposure time (~ 100 ms), the OTF of the optical system together with atmospheric turbulence is

$$H(u, v) = H_{\text{op}}(u, v) \exp\{-K(u^2 + v^2)^{5/6}\} \quad (56)$$

where $H_{\text{op}}(u, v)$ is the OTF of the optical system in the absence of atmospheric turbulence, and K a constant. For short exposure time (~ 1 ms), the PSF and the OTF of atmospheric turbulence look random. The ensemble average of the OTF (after elimination of linear phase factors) is

$$\overline{H(u, v)} = H_{\text{op}}(u, v) \exp\left\{-K(u^2 + v^2)^{5/6} \left[1 - \left(\frac{u^2 + v^2}{f^2}\right)^{1/6}\right]\right\} \quad (57)$$

under near field conditions ($D \gg (L\lambda)^{1/2}$, where D is the diameter of the entrance pupil of the optical system, L the length of propagation path through the turbulent medium, and λ the wavelength of light), where f is the cutoff frequency of the optical system. Under

far-field conditions ($D \ll (L\lambda)^{1/2}$), the ensemble average becomes

$$\overline{H(u, v)} = H_{\text{op}}(u, v) \exp\left\{-K(u^2 + v^2)^{5/6} \left[1 - \frac{1}{2} \left(\frac{u^2 + v^2}{f^2}\right)^{1/6}\right]\right\}. \quad (58)$$

We note from (56)–(58) that at spatial frequencies close to the cutoff frequency of the optical system, the long exposure OTF is considerably smaller than the short-exposure average. Therefore, short-exposure pictures are preferred to a long-exposure one.

We mention in passing that the atmosphere, in addition to being turbulent, also scatters and absorbs light. These latter effects cause a decrease in image contrast [86], [43], [123].

3) *Edge Analysis:* If we have reason to believe that the original scene contains a sharp point, then the image of that point gives us the PSF or impulse response of the imaging system. For example, in a picture of Jupiter and its satellites, we can consider the image of one of the satellites as the degrading impulse response and devise a corresponding inverse filter to improve the quality of the Jupiter image.

Usually, the original scene will probably not contain any sharp points. However, it is quite likely that it contains sharp edges. If the degrading system is circularly symmetric, then it is well known that we can derive the impulse response from an edge response [41]. It is less well known but nonetheless true that if the degrading system is not circularly symmetric, we can still estimate the impulse response, if we know the responses of edges in many different directions. This latter problem turns out to be mathematically equivalent to the problem of reconstructing three-dimensional structures from two-dimensional projections [58], [220].

Let $h(x, y)$ be the PSF or impulse response of the degrading system, and let $g(y)$ be the response of the system due to an input $\delta(y)$ which is an impulse sheet on the x axis representing a line input. We have used $\delta(\cdot)$ to denote the Dirac delta function. Then it is readily shown that the OTF, which is the two-dimensional Fourier transform of $h(x, y)$, and the one-dimensional Fourier transform of $g(y)$ are related by

$$H(0, v) = G(v). \quad (59)$$

Since the choice of the directions of the x and y axes is really arbitrary, we conclude that the one-dimensional Fourier transform of the response of the system due to an input line at an angle θ from the x axis is equal to the OTF evaluated along a line passing through the origin and at an angle θ from the v axis. Therefore, we can get the OTF of a system, if we know the responses of the system due to input lines at all directions. We note finally that the line response is the derivation of the edge response.

One major obstacle in this method of estimating the impulse response is the film grain noise in the degraded image. The effects of noise on the determination of the line spread function (and its one-dimensional Fourier transform) from measured edge traces, and various methods of smoothing the noise have been studied by numerous researchers [125]–[127], [35], [230], [38], [39], [159], [180], [87].

4) *Image Segmentation:* The method of estimating the OTF of LSI degrading systems which we are going to describe now was inspired by the very interesting work done by Prof. Stockham, Jr., Computer Science Department, University of Utah, on the restoration of old Caruso recordings. The mathematics is quite similar to the multiframe processing scheme we discussed in Section II-C4-1.

Suppose we divide the original into M regions (all identical in size) and denote the light intensity distribution in region i by $f_i(x, y)$; $i = 1, 2, \dots, M$; where (x, y) are spatial coordinates. Let $p_i(x, y)$; $i = 1, 2, \dots, M$; be the light intensity distributions of the corresponding regions in the degraded image. Assuming the extent of the de-

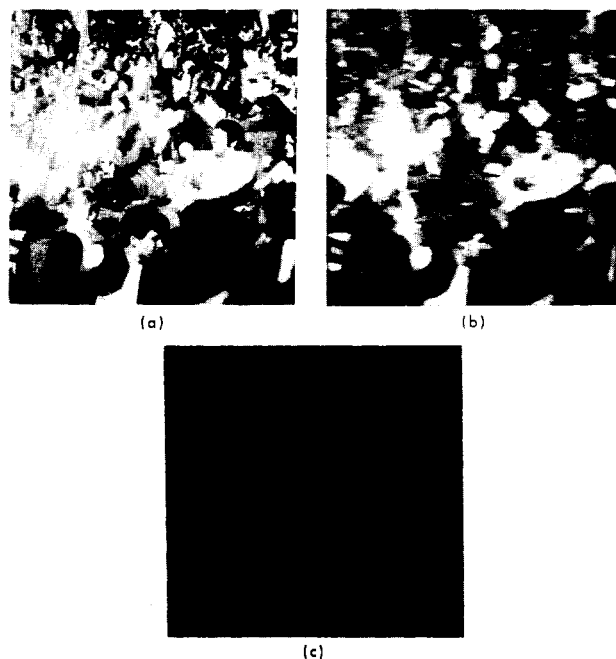


Fig. 3. (a) Original scene, digitized to 256×256 samples, with 256 brightness levels per sample. (b) Degraded image, obtained from the original scene by smearing (16-point average) in the horizontal direction. (c) Estimated impulse response of the degrading system. The intensity of the display is proportional to the magnitude of the impulse response.

grading impulse response $h(x, y)$ is small compared to that of each region of the image, we have, except for edge effects,

$$P_i(x, y) = f_i(x, y) \otimes h(x, y), \quad i = 1, 2, \dots, M \quad (60)$$

where \otimes denotes convolution. Taking the Fourier transform of both sides of (60), we get

$$P_i(u, v) = F_i(u, v) H(u, v), \quad i = 1, 2, \dots, M \quad (61)$$

where we have used capital letters to denote the Fourier transforms. Taking the product over i , we get

$$\prod_{i=1}^M P_i(u, v) = \left[\prod_{i=1}^M F_i(u, v) \right] H^M(u, v)$$

or

$$H(u, v) = \left[\prod_{i=1}^M P_i(u, v) \right]^{1/M} / \left[\prod_{i=1}^M F_i(u, v) \right]^{1/M}. \quad (62)$$

If the light distributions in the M regions of the original scene vary sufficiently fast and are sufficiently different from one another, then we expect that the denominator at the right-hand side of (62) is approximately a constant (i.e., independent of u and v). Therefore, we can estimate $H(u, v)$ and hence $h(x, y)$ from $P_i(u, v)$ which we can calculate from the degraded image.

In most cases we shall encounter, it is probably reasonable to assume that the phase angle of $(\prod_{i=1}^M F_i)^{1/M}$ is approximately constant. However, in most images, the magnitude of $(\prod_{i=1}^M F_i)^{1/M}$ will not be constant. Therefore, we have to guess at the form of $|(\prod_{i=1}^M F_i)^{1/M}|$ in order to obtain an estimate of H .

We have done some preliminary investigations on this method of estimating impulse responses on a digital computer [62]. A fast-varying picture [Fig. 3(a)] was taken as the original. We degraded this picture in the computer by smearing it in the horizontal direction. Each point of the degraded image [Fig. 3(b)] was the average of 16 points in the original. The impulse response of the degrading

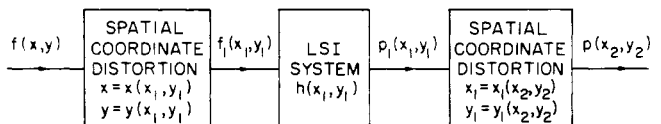


Fig. 4. A special class of LSV systems.

system was then estimated from the degraded image by using (62), assuming that the denominator was a constant. The image was divided into 16 regions, each containing 64×64 points. The result is shown in Fig. 3(c), which is rather close to the actual impulse response.

We are currently looking into ways of improving this method of estimating impulse responses, in particular, by being more careful in handling the phase angles of P_i and by applying results of statistical estimation theory.

E. Linear Shift-Varying (LSV) Degrading Systems

As mentioned earlier, some degrading systems (e.g., lens aberrations) can be modeled by the block diagram in Fig. 2 with the linear system shift-varying. Some aspects of shift-varying image formation were discussed by Cutrona [55], and Lohmann and Paris [148]. The output $p(x, y)$ and the input $f(x, y)$ of an LSV system are related by a superposition integral

$$p(x, y) = \int \int_{-\infty}^{\infty} k(x, y; \alpha, \beta) f(\alpha, \beta) d\alpha d\beta \quad (63)$$

where $k(x, y; \alpha, \beta)$ equals the output at (x, y) due to an input impulse at (α, β) . The restoration problem is: Find $f(x, y)$ from given $p(x, y)$ and $k(x, y; \alpha, \beta)$. That is we want to solve the linear integral equation (63).

Equation (63) can be solved if we can find a complete set of eigenfunctions for the kernel $k(x, y; \alpha, \beta)$. Unfortunately, in most cases of interest, we simply do not know how to find the eigenfunctions; we do not even know whether they exist. In theory, we can always find an approximate solution to (63) by brute force.

We digitize the equation to get a set of linear algebraic equations which we then solve for the samples of $f(x, y)$. However, in practice, the number of samples we have to take in an image is so large that the roundoff errors in calculation and the inherent noise (due to detector) in the degraded image (which we neglected in (63)) will swamp the numerical process.

1) *Piecewise—LSI Approach*: If the impulse response $k(x, y; \alpha, \beta)$ of an LSV system varies relatively slowly with the position (α, β) of the input impulse, then we can divide the input image into pieces and in each of these pieces approximate the LSV system by an LSI system. Then, in each piece we can use LSI inversion techniques. The question of how many pieces we shall cut the image into was discussed by Granger [79]. The mathematical theory behind the inversion of piecewise LSI systems (which involves Wiener-Hopf techniques) was studied by Robbins [178].

2) *A Special Class of LSV Systems*: In several cases of practical interest, the LSV systems belong to a special class depicted in Fig. 4. First, the input spatial coordinates are distorted according to

$$\begin{cases} x = x(x_1, y_1) \\ y = y(x_1, y_1) \end{cases} \quad (64)$$

so that the ideal image $f(x, y)$ becomes

$$f_1(x_1, y_1) = f(x(x_1, y_1), y(x_1, y_1)). \quad (65)$$

Then $f_1(x_1, y_1)$ is degraded by an LSI system with impulse response $h(x_1, y_1)$, yielding $p_1(x_1, y_1)$. Finally, the output spatial coordinates

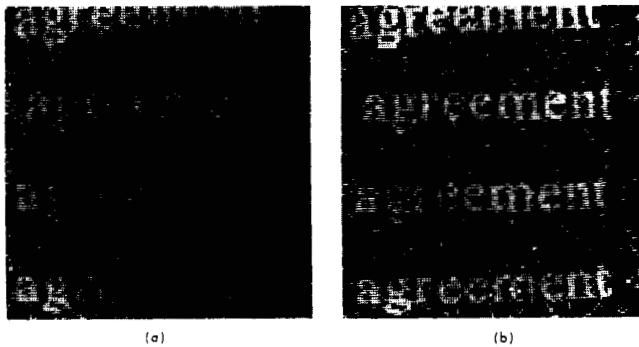


Fig. 5. Nonlinear noise reduction. (a) Noisy image. (b) Noise reduced.

are distorted according to

$$\begin{cases} x_1 = x_1(x_2, y_2) \\ y_1 = y_1(x_2, y_2) \end{cases} \quad (66)$$

yielding the final degraded image

$$p(x_2, y_2) = p_1(x_1(x_2, y_2), y_1(x_2, y_2)). \quad (67)$$

It should be obvious that if (64) and (66) have unique inverses, then the inversion of the special class of LSV systems depicted in Fig. 4 can be reduced to that of LSI systems.

One prominent example of an LSV degrading system that falls in this special class is the third-order coma aberration of a spherical lens [178]. Details on inverting the coma aberration are contained in a paper by Robbins and Huang in a forthcoming issue of the PROCEEDINGS on digital picture processing (July, 1972).

We note in passing that geometrical distortion [161], [36] can be considered as a special case of the class of LSV system depicted in Fig. 4—the case when only the first block is operating.

F. Nonlinear Processing

We have discussed so far mainly *linear* techniques of restoring linearly degraded images. It goes without saying that when the degrading system is nonlinear, it is natural to use nonlinear inverse filters. However, even when the degrading system is linear, nonlinear techniques are potentially more powerful. A general discussion on the use of optimum nonlinear filters in image restoration was given by Frieden [67].

1) *Elimination of Interference*: If we know the exact form of the interference, we can subtract it out from the image (on a digital computer, for instance). The most common type of interference in electrooptical imaging is sine-wave interference. In order to subtract a sine-wave interference out, we have to know both its amplitude and its phase. If the phase is not known, we can use a notch filter to eliminate the particular frequency component corresponding to the interfering sinewave [161]. It is important that this notch filter should have a linear phase so that it will not distort the image.

2) *Noise Reduction*: We give several examples of the use of nonlinear techniques in reducing noise in an image. Fig. 5(a) shows a noisy image which arose from a particular digital coding scheme for efficient picture transmission [113]. The image here has only two levels of intensity—each point is either white or black. The noise consists of white points spreading randomly over the image. We can reduce the noise by eliminating (i.e., changing to black) isolated small groups of white points. For example, when we eliminate in Fig. 5(a) all isolated white-point groups of size less than 3 points, the picture in Fig. 5(b) was obtained.

Graham [78] devised a nonlinear scheme for reducing random noise in continuous-tone images. Essentially, he considered any

image point which is sufficiently different from its neighbors a noise point, and replaced it by a local average. The scheme was tried on television pictures with some success.

The optimum least-mean square LSI filter for noise reduction can be obtained by setting $H(u, v)=1$ in (9). Bose [40] developed a procedure for obtaining optimum (least mean-square) nonlinear shift-invariant filters. However, because of its complexity, one is yet to see it applied to images.

3) *Contrast Enhancement*: If the contrast of an image is poor because of an excessive uniform background, we can remove part of the background by subtracting a constant from each image point.

Sometimes the image has poor contrast because it went through a nonlinear amnesic shift-invariant operator, such as the *H-D* curve of a film. If this operator has an inverse, then we can improve the contrast by applying the inverse operator to the image on a digital computer.

More generally, the image may have gone through a nonlinear amnesic shift-variant operator. Such is the case when we use a television camera tube which has a nonuniform field. Then each image point has to be treated with its own particular inverse operator. This was done by Nathan [161] on Moon and Mars pictures transmitted back to earth from satellites.

4) *Crispening*: Oftentimes we want to make an image appear sharper. One way to do this is to pass the image through a two-dimensional high-pass filter and thereby emphasize the high-frequency components of the image. Since noise is always present in an image, we have to be careful not to emphasize in the frequency range where the noise is larger than the signal.

Stockham [165] has shown experimentally that one can crisp much better if one compresses the dynamic range of the image logarithmically before the high-pass filter and then expands it exponentially afterwards. This can be explained heuristically by noting that the brightness of an image is approximately the product of the illumination $I(x, y)$ and the reflectance of the object $R(x, y)$. Taking the logarithm makes the two factors additive.

$$\log IR = \log I + \log R. \quad (68)$$

Therefore, the details of the object can be crisped more or less independently of the illumination.

An example of crispening using this technique is shown in Fig. 6. For computational convenience, we replaced the logarithm by the square root function (which has similar characteristics). The square root of the original image in Fig. 6(a) is shown in Fig. 6(b) which has a Fourier transform whose magnitude is displayed in Fig. 6(c). A high-pass filter was applied to the image in Fig. 6(b) to get the image shown in Fig. 6(e), the magnitude of whose Fourier transform is displayed in Fig. 6(d). Finally, the image in Fig. 6(e) was squared to get the enhanced image shown in Fig. 6(f).

III. EFFICIENT PICTURE CODING

A. The Problem

The transmission of images finds applications in many diverse fields, such as picturephone, computer-computer and man-computer communications, and remote sensing (in space exploration, reconnaissance, biomedical engineering, and other areas). In still other cases, although image transmission to a remote location is not required, one does need to store the images for future retrieval and analysis. Some examples are the filing and storage of engineering drawings, finger prints, and library books and journals.

The trend in image transmission and storage is to use digital instead of analog techniques. This is because of the many inherent advantages of digital communication systems [144] in the case of transmission, and the flexibility and ubiquity of digital computers in

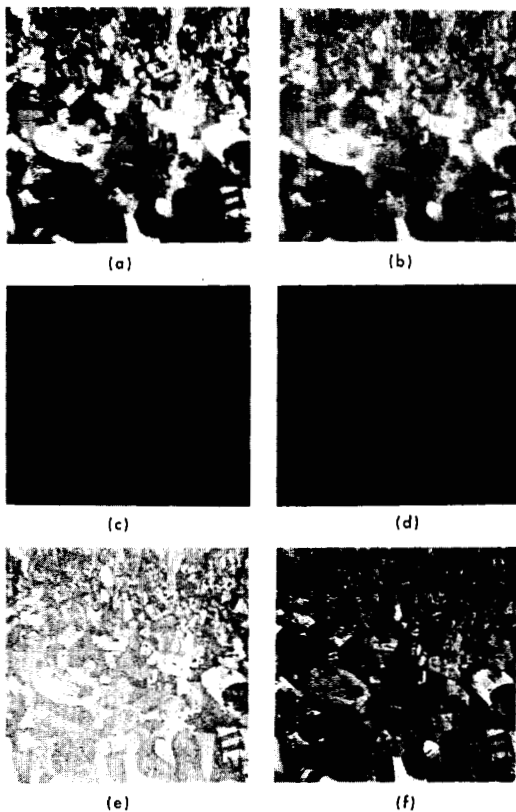


Fig. 6. Image crispening. (a) Original image $f(x, y)$. (b) $\sqrt{f(x, y)}$. (c) Magnitude of the Fourier transform of $\sqrt{f(x, y)}$. (d) Magnitude of the Fourier transform of \sqrt{f} multiplied by the frequency response of a high-pass filter. (e) $\sqrt{f(x, y)}$ high-passed. (f) Square of the high-passed \sqrt{f} .

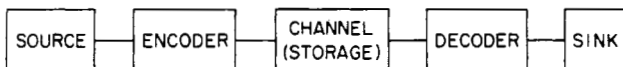


Fig. 7. A general block diagram for a transmission (storage) system.

the case of storage. In both cases, one major advantage of digital over analog techniques is that the errors are much easier to control for the former.

Since images generally contain a large amount of information, a common problem one encounters in the digital transmission and storage of images is that the required channel or storage capacity is often excessive. It is desirable and sometimes mandatory to find ways to reduce this capacity requirement. The reason that this capacity reduction is possible is twofold. First, there is statistical redundancy in images: image points which are spatially close to each other tend to have nearly equal brightness levels. Secondly, there is psychovisual redundancy in images: one can intentionally destroy some of the information contained in an image without causing a loss in its subjective quality. Many schemes have been devised in which some of the statistical and psychovisual redundancies of images are removed to reduce the channel (storage) capacity requirement [226].

1) *Rate-Distortion Theory*: A general block diagram for a signal transmission (storage) system is shown in Fig. 7. The source puts out signals, which in our case are images. The signals are transferred to the sink, in our case a human observer, via the channel or storage. The encoder transforms the source images into a form suitable for the channel or storage, and the decoder transforms the output from the channel or storage into a form suitable for the human observer. The problem a system engineer has at his hands is to optimize this system: Given a source, a sink, and a fidelity criterion or distortion

measure for picture quality, how do we design the encoder and decoder so that the channel (storage) capacity requirement is a minimum? Alternately: Given a source, a sink, and a channel (storage), how do we design the encoder and decoder so that the quality of the image reaching the sink is maximized?

The ideal mathematical framework for our optimization problem is Shannon's rate-distortion theory [196], [27]. The main result of this theory states that: For a given source and a given fidelity criterion or distortion measure D , there exists a function $R(D)$, called the rate of the source, such that we can transfer our signal to the sink with a distortion as close to D as we wish as long as the channel (storage) capacity C is larger than $R(D)$, and this is impossible if $C < R$.

There are, however, considerable difficulties in trying to apply the rate-distortion theory to practical problems. First, in order to calculate the rate R , we need to have a realistic mathematical model (in statistical terms) of the source and a mathematical expression of the distortion measure D which agrees reasonably well with subjective judgment. Both of these are yet to be found. Second, even if we should find a realistic source model and a good distortion measure, they would probably be so complicated that we would have great difficulty in calculating the rate R analytically. Third, the rate-distortion theory tells us only what is the best we can do; it does not tell us in detail how to do it.

If mean-squared error is used as a fidelity measure, and if the image is modeled as a Gaussian random process, then one can compute the rate-distortion function in a fairly simple way [133]. This result has been extended to the weighted squared error criterion [183] and to contain classes of non-Gaussian processes [184]. A similar calculation can be made if the coding is done on a single scanning line [185].

It is interesting to note that the performance of realizable systems, such as feedback encoders and transformational coding comes very close to this bound [57], [215].

2) *A Practical System Layout*: In practice, instead of the general block diagram of Fig. 7, we prefer to work with a more detailed layout as shown in Fig. 8. A two-dimensional image is first spatially filtered, and then sampled in space and quantized in brightness. The psychovisual and statistical encoders remove, respectively, some of the psychovisual and statistical redundancies in the digitized image. The error-detection-and-correction encoder adds redundancy into the binary sequence representing the coded image to protect it from channel (storage) noise. The output binary sequence of this encoder is transformed by the modulator into waveforms suitable for transmission through the channel (or putting into storage). On the other side of the channel (storage), the demodulator and the decoders try to recover the best they can the output of the quantizer. Finally, the two-dimensional (spatial) post-filter smoothes out the recovered digital image into a continuous image for viewing by human observers.

The operations of the filters, the sampler, the quantizer, and the psychovisual and statistical coders are based on the properties of the source: they are called source coding. The operations of the error-detection and-correction coders and the modem (modulator and demodulator) are based on the properties of the channel (or storage): they are called channel coding. In the remainder of this chapter, we shall phrase our discussions in terms of image transmission, although most of the results apply to image storage as well.

Since all the blocks in Fig. 8 interact with each other, it is an impossible task to optimize the total system. One can only hope to design a good system instead of an optimum one, and to do so is as much an art as a science.

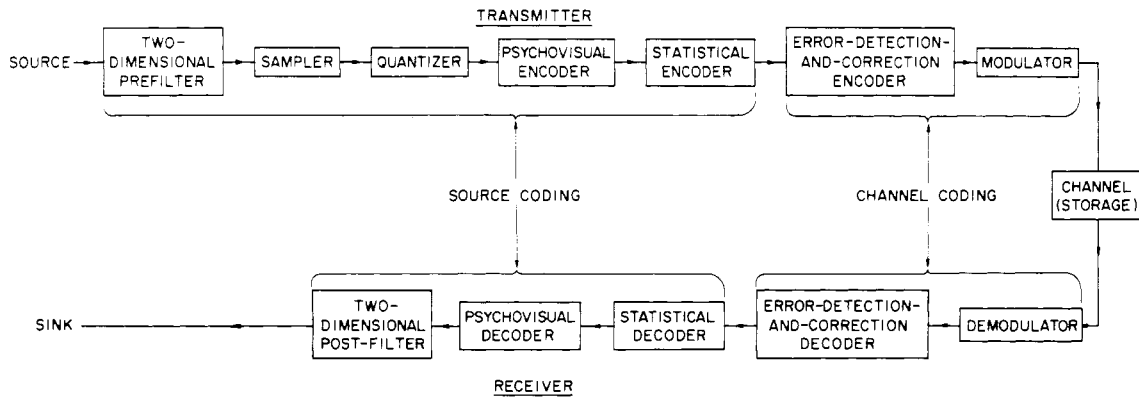


Fig. 8. A practical block diagram for an image transmission (storage) system.

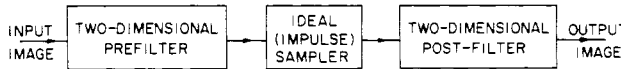


Fig. 9. The sampling process.

B. Image Digitization

1) *Sampling*: To concentrate on the sampling process, let us consider the simplified subsystem depicted in Fig. 9. With respect to this system, the basic question is: For a fixed number of samples per image frame, how should we choose the pre-filter and post-filter to optimize the output image quality?

Let the picture be sampled at a square array of points. Peterson and Middleton [169] showed that, for a fixed number of samples per frame pre- and post-filtering with two-dimensional ideal low-pass filters (whose cutoff frequencies are chosen to avoid aliasing) gives the least mean-square difference between the output of the post-filter and the input to the pre-filter. Subjective tests [112] indicated that these same filters also give reconstructed pictures with the best subjective quality in the case of very low resolution (64×64 samples per frame) systems.

For higher resolution systems (256×256 samples per frame), high-spatial-frequency accentuation at the post-filter seems to improve the output image quality; however, no extensive subjective tests have been done to verify this. Note that to obtain a received image with resolution comparable to that of present-day U. S. commercial television pictures, about 500×500 samples per frame are required.

2) *Quantization*: To each input sample (with a continuous brightness range) the quantizer assigns a discrete level. The quantization can be either uniform or nonuniform. If uniform quantization is used, about 5 to 8 bits per sample or 32 to 256 brightness levels (depending on the S/N of the original, the viewing conditions, etc.) are required to eliminate artificial contours (the so-called quantization noise). One can save about 1 bit per sample by using logarithmic quantization to take advantage of the properties of human vision (Weber-Fechner law).

Some examples of uniformly and logarithmically quantized images are shown in Figs. 10 and 11. The original image used in these examples contains a cameraman as the central object with grass and sky as background, and has a S/N (peak signal to rms noise ratio) of about 40 dB before quantization and a resolution of 256×256 sample points.

C. Redundancy Reduction

1) *Statistical Coding*: To transmit a digitized image by direct PCM requires $N = L \times L \times B$ bits per frame, where $L \times L$ is the num-

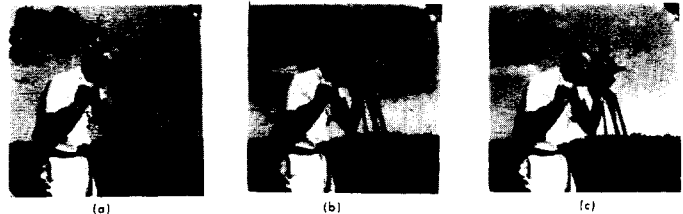


Fig. 10. Images uniformly quantized to various numbers of levels (256×256 samples per frame). (a) 2 bits or 4 levels. (b) 3 bits or 8 levels. (c) 5 bits or 32 levels.

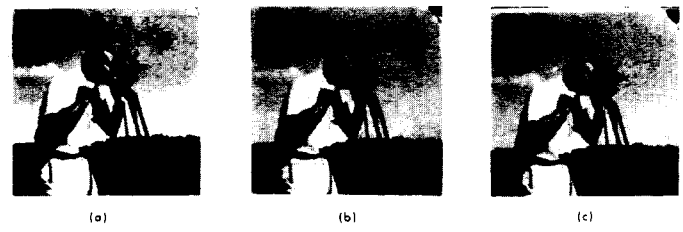


Fig. 11. Images logarithmically quantized to various numbers of levels (256×256 samples per frame). (a) 2 bits or 4 levels. (b) 3 bits or 8 levels. (c) 5 bits or 32 levels.

ber of samples per frame and B the number of bits per sample (2^B being the number of discrete levels used for the brightness of each sample). Since the channel capacity requirement increases with an increase in the number of bits used to represent the image, it is the purpose of the psychovisual and the statistical encoders (Fig. 8) to reduce the number of bits needed to characterize the digitized image. We shall first take up statistical coding.

We can characterize a digitized image by a sequence of messages. The messages can be, for example, the brightness levels of each individual sample. Or, each message may contain the brightness levels of a pair of neighboring samples. Still a third example is that the messages may be first differences of adjacent samples along each horizontal line. There are many ways to choose our messages, the only requirement being that we should be able to reconstruct the digitized image from the sequence of messages.

For a particular choice, let the possible messages by m_1, m_2, \dots, m_n ; and let the probability distribution of these messages (over the class of digitized images we are interested in) be p_1, p_2, \dots, p_n . The main idea in statistical coding is to use variable-length binary codewords for the messages, using short codewords for the more probable messages and longer codewords for the less probable ones so that on the average we will have a small number of bits per message. Shannon's theory [196] tells us that we can always find a code such that

the average number of bits per message r satisfies the inequality

$$H \leq r \leq H + 1 \quad (69)$$

where the entropy H is by definition

$$H \equiv - \sum_{i=1}^n p_i \log_2 p_i. \quad (70)$$

The simple and elegant procedure of Huffman [115] guarantees that we will get a code with the minimum r .

The entropy H for a probability distribution is maximum when all p_i are equal, and is minimum when all p_i but one are zero. Generally speaking, the more nonuniform or peaky a probability distribution, the smaller its entropy. Therefore, in order to do effective statistical coding, we should choose a message set which has a peaky probability distribution.

2) *Psychovisual Coding*: If the received picture is to be viewed by humans, then one can take advantage of the properties of human vision. Here, the purpose is to distort the picture in such a way that it can be described by a smaller number of bits; however, the distortion is not great enough to be noticeable or objectionable to the human viewer. Psychovisual encoding, then, can be considered as an operation to derive a sequence of messages from the digitized image such that these messages require less channel capacity to transmit than the original digital image and that from these messages we can reconstruct a reasonable replica of the original digital image. Statistical encoding can, of course, be applied to the output messages of a psychovisual encoder to reduce their statistical redundancy.

We shall see that it is in psychovisual coding that we can hope for large amounts of redundancy reduction. Indeed, without taking advantage of the psychovisual properties of human vision, we would have had neither movies nor black-and-white and color television. The discrete-frame approach of movies and television (around 30 frames/s) is satisfactory because of the limited resolution of the temporal response of the human vision. Color television is possible because we can synthesize any subjective color by using a finite (3 or 4) number of color components. In both cases, a continuum is reduced to a finite discrete set: the bandwidth compression or redundancy reduction ratio is infinite.

Many redundancy reduction schemes have been developed and studied by various research groups, especially at the Bell Telephone Laboratories. One of the most simple and practical schemes is perhaps differential PCM. However, since our paper concerns image processing, in the remainder of this section we shall describe only two schemes which make use of truly two-dimensional processing techniques.

D. Contour Coding

1) *The Contours of Images*: If a drawing consists of a relatively small number of thin black lines on a white background the important points are obviously the black ones since the entire image may be constructed only from the black points and there are relatively few of them. In the more general case of a continuous-tone picture, the significant points must be selected in a more complicated manner. They are usually points of sharp brightness change. From the statistical point of view, these points are significant because they are highly correlated and thus can be efficiently coded. From the perceptual point of view, points of sharp brightness change are significant because they are usually associated with the outlines of objects.

In the reconstruction of images from outlines it is obvious that in the case of graphical, i.e., two-level data, the image may be re-created exactly from the outline information since all that is necessary is to fill in the spaces between the outlines with black. It turns out that continuous-tone images may also be recreated exactly from the outlines provided that they also contain information about the

spatial gradients of the image. Just as a function of single variable can be reproduced to within an additive constant from its derivative, a function of two variables, i.e., an image, can be recovered from its gradient [187]. The outlines are generally found to consist of connected series of points having gradients significantly different from zero. Thus if all the significant outlines are transmitted all the significant gradient information will be available for picture reproduction.

An alternate and less efficient way of characterizing continuous-tone pictures in terms of outlines or contours may also be mentioned here. Assume that the picture has been sampled in space and quantized in brightness. Then the picture can be considered as consisting of areas, each area containing a connected group of points with the same brightness level. We can characterize the picture completely by specifying the boundary points and the brightness levels of all the areas. This and related methods of picture coding, such as bit-plane encoding [208], suffer from the fact that many of the area boundaries do not correspond to the outlines of natural objects, but are merely artifacts of the quantization process. We might mention in this connection that Baer [31] looked into the efficient coding of the medial axis transforms of picture areas, with rather disappointing results.

2) *Transmission of Contour Information*: The information which needs to be transmitted about the outlines or contours in an image consists simply of the location of the contour points in the case of graphical data or the location plus gradient information or area brightness levels in the case of continuous-tone images.

Several coding techniques are available for transmitting contours [189], the most natural among which is perhaps to trace the contours directly. We first transmit the coordinates of an initial contour point. Then we trace the contour. In a digitized picture, each picture point has only 7 neighboring points. Therefore, once we are on a contour, it takes at most 3 bits to indicate the next contour point. In the case of continuous-tone images where gradient information must also be transmitted, one may also transmit the value of the gradient at the initial contour point and incremental information permitting the calculation of the gradient at the rest of the points.

3) *Coding of Typewritten English*: We give an example of the contour coding of typewritten English characters.

Based on a standard table of frequencies of the English letters, it was calculated that the average number of contours per letter is 1.5. At a resolution of 300 points/in, the number of contour points of the lower case elite type letters were counted, and the average number of contour points per letter was calculated to be 120 points/letter. On a standard single-space typewritten page, each letter occupies 1/12 by 1/6 in or, at 300 points/in, $25 \times 50 = 1250$ points.

We now estimate the compression ratios for the contour coding schemes on a single-letter basis. The compression ratios for an ordinary typewritten page, which contains margins and spaces, would be considerably higher. For direct contour tracing using 3 bits per contour point and 11 bits for the initial contour point, the compression ratio is:

$$\frac{1250}{11 \times 1.5 + 3 \times 120} \approx 3.$$

We should point out that the compression ratios of most coding schemes depend critically on image resolution [189], [108]. For instance, in the above numerical example, we have assumed a resolution of 300 points/in. If the resolution is increased to 1000 points/in, the compression ratio becomes 10.

4) *Continuous-Tone Pictures—Gradient Approach*: The contour coding of continuous-tone pictures using gradient information will now be described in some detail. This scheme takes advantage of the

fact that the human eye tends to emphasize edges (abrupt changes in brightness) in a picture but is relatively insensitive to the amount of changes in the brightness over edges; on the other hand, in areas where the brightness changes slowly, quantization noise is easily discernable. Therefore, edges and slowly varying part of a picture were treated differently.

The original image $s(x, y)$ is passed through a two-dimensional low-pass filter. If the bandwidth of the low-pass filter is 1/100 of that of the original image $s(x, y)$, then the output $a(x, y)$ needs to be sampled only 1/100 as often as $s(x, y)$; each sample of $a(x, y)$ still has to have 6 bits to avoid quantization noise. The image $s(x, y)$ is also passed through a gradient operator, since $|\nabla s|$ is large at the edges in the image this signal contains mainly edge information. It can be shown readily that if the low-frequency part $a(x, y)$ and the gradient components $\partial s/\partial y$ and $\partial s/\partial x$ are sent exactly (and if the channel is noiseless), then one can synthesize the high-frequency part, viz., $s(x, y) - a(x, y)$, exactly, by passing the gradient components through appropriate two-dimensional linear filters, and the original picture will be reproduced exactly [187a]. Graham worked on the problem of how to approximate the gradient so that we can achieve a large amount of reduction and also at the same time obtain good received pictures [77]. He considered as edge points all points whose gradients had magnitudes greater than a certain threshold. The gradients of these edge points then were transmitted by contour tracing. For each continuing contour point, he transmitted the changes in contour direction, gradient direction, and gradient magnitude using a Huffman code [115]. From the probability distributions of these quantities, he estimated the compression ratios of 4 to 23 (depending on picture complexity) could be achieved on 256×256 -point 6-bit (64-brightness level) pictures.

Fig. 12 illustrates this scheme. Note that a tremendous amount of redundancy reduction was possible using this scheme. However, the reconstructed image suffered from a loss of textures. This was because the textures are often high-frequency low-amplitude signals. They are on the one hand not included in the low-frequency part of the image, and, on the other hand, not large enough to pass the gradient threshold.

5) *An Operational Definition of Texture*: The shortcoming of Graham's contour coding schemes suggests the following operational definition of texture. We consider an image as the sum of three components: the low-frequency part, the edges, and the textures. The low-frequency part and the edges correspond, respectively, to the low-frequency part and the synthesized high-frequency part (from approximate gradient information) in Graham's scheme. The texture component is then by definition what is left over in the original image after we subtract from it the low-frequency part and the edges. We should mention that much work on texture has been done recently by Rosenfeld and his colleagues at the University of Maryland [11].

E. Transformational Coding

1) *Linear Transformation and Block Quantization*: The results of the rate-distortion theory strongly suggest that the use of linear transformation and block quantization might be quite efficient in coding data. Such an approach was analyzed by Kramer and Mathews [136] and Huang and Schultheiss [105]. The basic scheme is as follows. A block of N data samples x_i are linearly transformed into y_i by an $N \times N$ matrix A . The y_i are quantized and transmitted. At the receiver, the quantized y_i are transformed by another $N \times N$ matrix B into z_i . For a given bit rate, the matrices A and B are chosen to minimize the mean-square error between z_i and x_i . It turns out that the optimum matrix A consists of the eigenvectors of the correlation matrix of the samples x_i , and the optimum matrix B is the inverse of A . It appears, however, that a much simpler type of matrices, the so-called Hadamard matrices work almost as well as

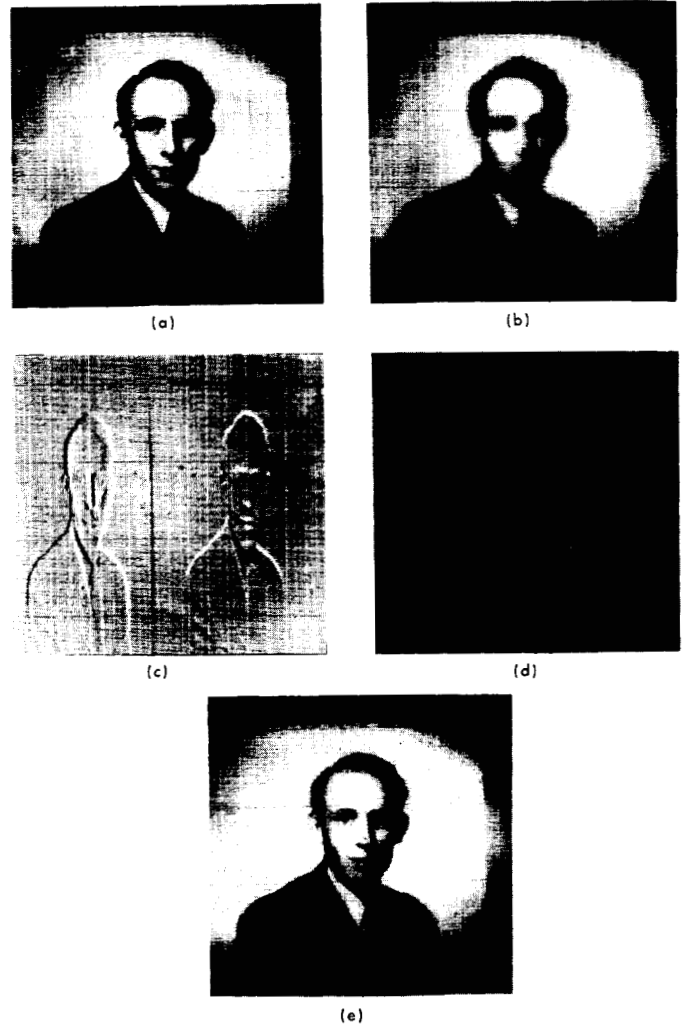


Fig. 12. The contour coding scheme of Schreiber and Graham. (a) Original (256×256 samples, 6 bits/sample). (b) Low-frequency part of the picture. (c) Gradients. (d) Synthetic highs. (e) Reconstruction (0.3 bit/sample).

the optimum [174], [85]. A Hadamard matrix contains only +1 and -1 as its elements, and is orthogonal. Except for a scalar factor, it is its own inverse.

2) *Hadamard Transform Coding*: The application of Hadamard matrices to block quantizing images was studied by Huang and Woods [114], [229]. Let us assume, for simplicity, that the sampled image is divided into 2×2 blocks. Call the intensities of the 4 samples in a block x_1, x_2, x_3 , and x_4 . These intensities are transformed into y_i by a 4×4 Hadamard matrix:

$$\begin{pmatrix} y_1 \\ y_2 \\ y_3 \\ y_4 \end{pmatrix} = \begin{pmatrix} 1 & 1 & 1 & 1 \\ 1 & -1 & 1 & -1 \\ 1 & 1 & -1 & -1 \\ 1 & -1 & -1 & 1 \end{pmatrix} \begin{pmatrix} x_1 \\ x_2 \\ x_3 \\ x_4 \end{pmatrix}. \quad (71)$$

Since in a typical image neighboring samples tend to have equal intensities, y_i ($i \neq 1$) tend to be very small. Therefore, in quantizing the y_i , we use more bits for y_1 and fewer bits for y_2, y_3 , and y_4 , hoping that we may end up with a small average number of bits per sample and yet get a good quality reconstructed image.

This scheme was applied to several images, and various block sizes were tried. It was found that for a given average bit rate, the use of a large block size tended to make the degradation in the reconstructed image appear as random noise, while the use of a small block size made the degradation appear in the form of discon-



Fig. 13. Hadamard block quantization (block size = 8×8). Average number of bits per sample. (a) 1. (b) 2. (c) 3.



Fig. 14. Hadamard block quantization (block size = 16×16). Average number of bits per sample. (a) 1. (b) 2. (c) 3.

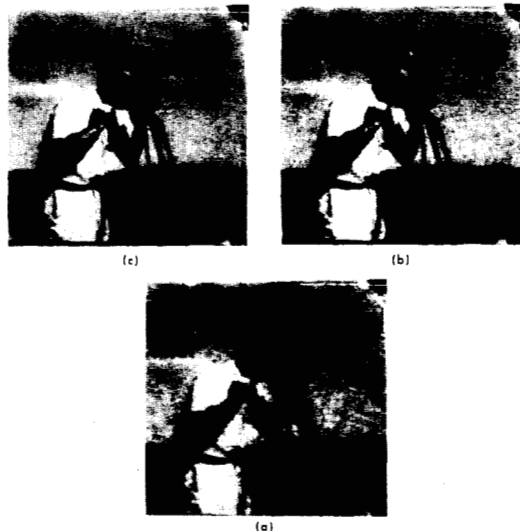


Fig. 15. Hadamard block quantization (block size = 1×256). Average number of bits per sample. (a) 1. (b) 2. (c) 3.

tinuities at block boundaries. Some results (using square blocks) are shown in Figs. 13 and 14 (all pictures contain 256×256 samples). Note that with 3 bits per sample, the picture quality becomes as good as that of 6-bit originals.

In implementing image coding schemes in real time, it is easier to work along a scan line rather than in two dimensions. Therefore, the Hadamard block quantization scheme was also tried with one-dimensional blocks. Some results are shown in Fig. 15 (all pictures contain 256×256 samples). Note that the 3-bit picture is as good as the 3-bit picture using 16×16 blocks, but the 2-bit and 1-bit pictures have inferior quality when compared to the corresponding pictures using 16×16 blocks.

We mention in passing that similar results of Hadamard image coding have been obtained independently by other researchers [140], [85]. Pratt, Kane, and Andrews [172] studied the coding of the Hadamard transform of the entire image. The results thus obtained appeared not as good as those obtained from coding small pieces of the image.

3) Other Schemes: In the preceding section, we described a scheme of block quantizing images using Hadamard transforms. It turns out that we can also achieve good results using Fourier instead

of Hadamard transforms. Furthermore, we can encode the transformed variables in many different ways other than dividing them into groups and use a fixed number of quantization levels for each group. In short, a variety of transformational coding schemes exist. We might mention that a piecewise Fourier-transform coding scheme of Anderson and Huang [26] gives good quality pictures at about 1 bit per point on the average.

IV. OPTICAL IMAGE PROCESSING TECHNIQUES

A. Preliminaries

In Sections II and III, we have discussed some of the important mathematical operations we often want to perform in image processing. Some of these operations are linear; e.g., Fourier and Hadamard transformation, linear filtering, and correlation. Others are non-linear; e.g., contour tracing. In Sections IV–VI, we shall describe the implementation of these mathematical operations using optics, digital computers, and special electrooptical devices.

B. Fourier Transformation

The main uses of coherent optical systems in image processing have been Fourier transformation and linear filtering. These operations are possible because of the Fourier-transforming property of a lens [56], [74], [199]. If a film transparency with amplitude transmission $g(x, y)$ is placed in the front focal plane of a lens, where x and y are the spatial coordinates of the front focal plane, and is illuminated with collimated monochromatic light, then the amplitude of the light at the back focal plane of the lens will be

$$G(2\pi\xi/\lambda f, 2\pi\eta/\lambda f) = G(u, v)$$

the Fourier transform of $g(x, y)$, where u and v are frequency variables, ξ and η the spatial coordinates of the back focal plane, λ the wavelength of the light, and f the focal length of the lens.

It is to be noted that if we put a detector (e.g., film) at the back focal plane of the lens, we will detect $|G|^2$ —the phase information is lost.

C. Linear Filtering and Correlation

Linear filtering can be performed by first obtaining the Fourier transform of the input image $g(x, y)$ using a lens as described in the preceding subsection, and then putting a transparency, with amplitude transmission $H(u, v)$ in the back focal plane of the lens, and using a second lens whose front focal plane coincides with the back focal plane of the first lens. Then at the back focal plane of this second lens, the light amplitude will be $p(\alpha, \beta) = g(\alpha, \beta) \otimes h(\alpha, \beta)$ where α and β are the spatial co-ordinates, \otimes denotes convolution, and $h(\alpha, \beta)$ is the inverse Fourier transform of $H(u, v)$.

The cross-correlation function $R_{gk}(x, y)$ of two real functions $g(x, y)$ and $k(x, y)$ can be expressed in terms of a convolution

$$R_{gk}(x, y) = g(x, y) \otimes k(-x, -y). \quad (72)$$

Therefore, we can do the cross correlation by performing a linear filtering with $g(x, y)$ as the input and $k(-x, -y)$ as the impulse response of the filter.

We mention in passing that several alternative ways of performing linear filtering and correlation using coherent optics were described by Weaver *et al.* [224].

D. Making the Spatial Filter

In doing general linear (shift-invariant) filtering using the setup described in subsection C, the filter $H(u, v)$ can be complex. We can generate a complex filter by controlling both the density and the thickness of a film transparency. However, the control of film thickness is difficult. Fortunately, there are methods by which one can

perform complex filtering using film transparencies which have density variation only. We shall describe three such methods.

The first method, due to Vander Lugt [222], employs a phase modulation technique to embed the phase information of the filter in the density variation. Instead of using $H(u, v)$, which is complex, we use as our filter the real and positive function

$$H_1(u, v) = |H(u, v) + A \exp(jau)|^2 \quad (73)$$

where A and a are constants. Then, in the output plane, we get $g(x, y) \otimes h_1(x, y)$ where $h_1(x, y)$ is the inverse Fourier transform of H_1 . It is readily shown that $g \otimes h_1$ contains a term $g \otimes h$, which is the desired output, shifted a distance a away from the optical axis.

The second method due to Lohmann [45], [149], and the third method due to Lee [142]–[144] both produce sampled filters. Brown and Lohmann essentially generate on a digital computer a halftone image of the desired filter $H(u, v)$. The trick lies in the shifting of the position of the halftone dot to control the phase information. The computer-generated filter can be plotted on a Calcomp plotter and then photoreduced to produce a filter transparency of the appropriate size.

Lee uses a digital computer and a precision CRT scanner to generate a sampled filter on which each group of four samples represent one point of the desired complex filter; the intensities of the four samples being proportional to the positive real part, the negative real part, the positive imaginary part, and the negative imaginary part, respectively, of the complex value of the filter point.

Just as in the case of the Vander Lugt filter, when we use either the Lohmann filter or the Lee filter, the desired output will appear off the optical axis. Two examples of the use of Lee filters are shown in Fig. 16 (differentiation) and Fig. 17 (matched filtering).

E. Real-Time Operations

In a coherent optical Fourier transforming or filtering system, the input image and the filter are usually recorded on photographic (silver-halide) film transparencies. The development of photographic film is messy and time-consuming. Therefore, in order to operate the optical system in "real-time," i.e., to have the capability of changing the input and the filter very quickly, one has to search for a better medium than the photographic film. One needs a medium which can be modulated quickly by some form of energy (light, electron beam, sound, etc.), read at a visible wavelength, and be quickly erasable. One also requires that this medium be very sensitive, have high resolution and large dynamic range, and be fatigueless.

Such a medium has not yet been found. However, encouraging preliminary experiments have been done by various researchers with KDP crystals [171], photochromics [99], ultrasonic light-modulators [29], [157], photopolymers [182], and magneto-optical devices [51].

F. Other Optical Filtering and Correlation Schemes

It is possible to do linear filtering and correlation with non-coherent optics [155], [186], [221], [80] and partially coherent optics [52b]. However, they are much less flexible than the coherent case; in particular, the form of the filter function is rather restricted and cannot be specified arbitrarily.

Using polarized light and Polaroid Vectorgraph film, Marathay [152] developed a method of doing complex spatial filtering that yields filtered images on axis.

G. Matrix Multiplication

The basic concepts of doing matrix multiplication by coherent optics were discussed by Cutrona [55]. A more detailed analysis was carried out by Heinz, Artman, and Lee [96].

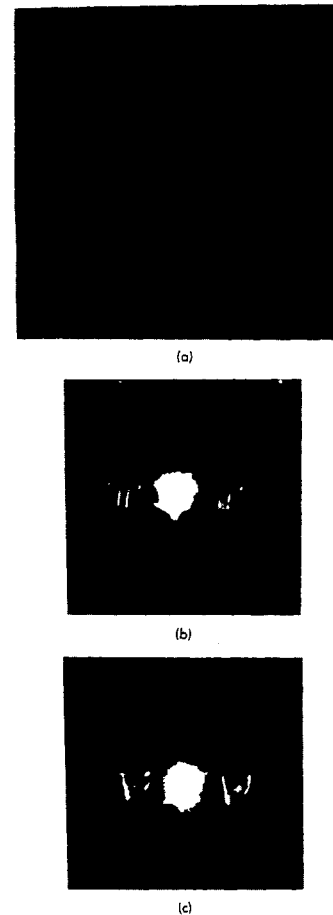


Fig. 16. Differentiation using a Lee filter. (a) Derivative filter. (b) Output pattern obtained using the letter "T" as input pattern. (c) Output pattern obtained using a sector of a circular disk as the input pattern.

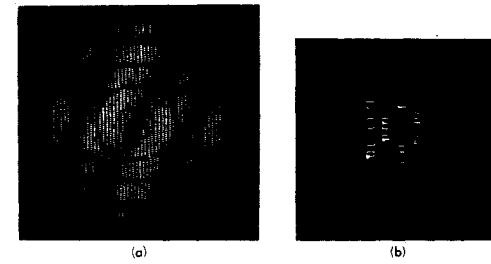


Fig. 17. Matched filtering using a Lee filter. (a) Matched filter for the letter "O." (b) Output pattern. Note that the input pattern appears in the center, while the desired output is off axis.

H. Holographic Subtraction

Bromley, Monahan, Bryant, and Thompson [44] developed a holographic technique by which two dissimilar optical fields can be subtracted to yield only their difference. The principle underlying this technique is that of optical interference between a holographically reconstructed field and a direct real-time one. One application of this technique is to detect changes between photographic transparencies of some scene taken at different times.

V. DIGITAL COMPUTER IMAGE PROCESSING TECHNIQUES

A. Fourier Transformation

To do any operation on a digital computer, the input image has to be sampled. If the input image contains N uniformly spaced samples, then it can be easily shown that one needs N samples for the Fourier transform. For the sake of simplicity, let us consider the one-

dimensional case. Let the values of the samples of the input, $g(x)$, be $g_0, g_1, g_2, \dots, g_{N-1}$ and those of the Fourier transform be $G_0, G_1, G_2, \dots, G_{N-1}$. Then

$$G_k = \sum_{j=0}^{N-1} g_j w^{-jk} \quad (74)$$

where

$$w = \exp [i(2\pi/N)]. \quad (75)$$

Equation (74) is a discrete approximation of the continuous Fourier integral, and can be written in matrix form:

$$[G] = W[g] \quad (76)$$

where

$$[G] = \begin{bmatrix} G_0 \\ G_1 \\ \vdots \\ G_{N-1} \end{bmatrix} \quad (77)$$

$$[g] = \begin{bmatrix} g_0 \\ g_1 \\ \vdots \\ g_{N-1} \end{bmatrix} \quad (78)$$

and

$$W = \begin{bmatrix} 1 & 1 & 1 & \cdots & 1 \\ 1 & w^{-1} & w^{-2} & \cdots & w^{-(N-1)} \\ 1 & w^{-2} & w^{-4} & \cdots & w^{-2(N-1)} \\ \vdots & \vdots & \vdots & \ddots & \vdots \\ 1 & w^{-(N-1)} & w^{-2(N-1)} & \cdots & w^{-(N-1)^2} \end{bmatrix}. \quad (79)$$

The samples of the Fourier transform can be obtained by carrying out the matrix multiplication of (76). To do this matrix multiplication directly, we need N^2 basic operations, a basic operation being defined as a complex multiplication plus a complex addition. To get each of the N output samples, we need N basic operations on the input samples. Therefore, the computer time required for the direct method is

$$T_d = kN^2 \quad (80)$$

where k is a constant, depending on the particular computer and the particular program.

An efficient method of digital Fourier analysis, which had been suggested by Good [71], was recently developed by Cooley and Tukey [53]. This method is based on the following theorem.

Let $N = r_1 \times r_2 \times \cdots \times r_n$, where r_1, r_2, \dots, r_n are positive integers. Then the $N \times N$ matrix W of (79) can be factored into n matrices:

$$W = W_1 W_2 \cdots W_n \quad (81)$$

where the $N \times N$ matrix W_i has only $r_i N$ nonzero elements.

It follows from this theorem that (76) can be written as

$$[G] = W_1 W_2 \cdots W_n [g]. \quad (82)$$

If we do the matrix multiplication step by step, multiplying W_n and $[g]$ first, then multiplying W_{n-1} and the product $W_n [g]$, etc., then the computer time required will be

$$T_c = k(r_1 + r_2 + \cdots + r_n)N. \quad (83)$$

The case $r_1 = r_2 = \cdots = r_n = 2$ offers important advantages for computers with binary arithmetic, both in addressing and in multiplication economy. In particular, the entire calculation can be performed within the array of $2N$ storage locations used for the input. (The input samples are in general complex, hence, each sample takes 2 storage locations.) For this special case the computer time required is, according to (83),

$$T_c = k2N \log_2 N. \quad (84)$$

We note that while in the direct method the computer time T_d is proportional to N^2 , in the Cooley-Tukey method, the computer time T_c is proportional to $N \log_2 N$. Therefore, for large values of N , considerable savings in computer time can be achieved by using the Cooley-Tukey algorithm.

For a typical computer, such as the IBM 7094, $k \approx 30 \mu s$. Using this figure we have

- for $N = 64 \times 64$, $T_d = 8$ min, $T_c = 30$ s
- for $N = 256 \times 256$, $T_d = 30$ h, $T_c = 1$ min
- for $N = 512 \times 512$, $T_d = 20$ days, $T_c = 5$ min
- for $N = 1024 \times 1024$, $T_d = 1$ year, $T_c = 20$ min.

The preceding estimates were made based on the assumption that the computer memory is large enough to store all the input samples. Also, the estimates do not include the input/output time.

In two dimensions, the discrete Fourier transform relation can be written as

$$G_{pq} = \sum_{p=0}^{M-1} \sum_{j=0}^{M-1} g_{pj} w^{-(pq+jk)} \quad (q, k = 0, 1, 2, \dots, M-1) \quad (84a)$$

or in matrix form

$$[G] = W[g]W \quad (84b)$$

where

$$[G] = \begin{bmatrix} G_{00} & \cdots & G_{0,M-1} \\ \vdots & & \vdots \\ G_{M-1,0} & \cdots & G_{M-1,M-1} \end{bmatrix} \quad (84c)$$

$$[g] = \begin{bmatrix} g_{00} & \cdots & g_{0,M-1} \\ \vdots & & \vdots \\ g_{M-1,0} & \cdots & g_{M-1,M-1} \end{bmatrix} \quad (84d)$$

and W is as defined in (79) except that N is replaced by M . Equation (84b) suggests that we can calculate the two-dimensional Fourier transform of $[g]$ by first calculating the one-dimensional transform of each row in $[g]$ and then in the resulting array calculating the one-dimensional transform of each column. It is easy to see that if we use the Cooley-Tukey algorithm to do the one-dimensional transforms in this procedure, then the time requirement of doing a two-dimensional transform is again given by (84), where $N = M^2$ is the total number of input samples.

The Cooley-Tukey algorithm is now commonly known as the Fast Fourier Transform or FFT [110]. A similar fast algorithm is available for the Hadamard transform [172], [1], [72].

B. Linear Filtering

Again, let us consider the one-dimensional case. Let g_i be the values of the input samples, and p_j those of the output. There are two

types of digital filters: 1) Nonrecursive filters—each output sample is a weighted sum of the input samples, viz.,

$$p_k = \sum_{j=0}^{M-1} A_j g_{k-j} \quad (85)$$

where A_j are constants. 2) Recursive filters—each output sample is a weighted sum of the input samples and the previously calculated output samples, viz.,

$$p_k = \sum_{j=0}^{M-1} b_j g_{k-j} + \sum_{i=1}^q c_i p_{k-i} \quad (86)$$

where b_j and c_i are constants. Equation (85) can be considered as a discrete approximation of the convolution integral; while (86), a difference equation corresponding to the differential equation describing the continuous linear filter.

There are various methods of designing both types of filters [37], [129], [70], which we will not go into here. It suffices to say that for a given continuous filter, approximating it by a recursive filter usually requires a smaller number of terms. On the other hand, error analysis is easier for nonrecursive filters.

We shall estimate the computer time requirement for digital filtering using a two-dimensional nonrecursive filter, the case of recursive filter being completely similar. Consider the filter operation:

$$p_{jk} = \sum_{a=0}^{m-1} \sum_{b=0}^{m-1} \{g_{j-a,k-b} h_{ab}\} \quad (j, k = 0, 1, \dots, n+m-1). \quad (87)$$

Assume the filter has $M=m \times m$ samples. Let the number of samples of the input image be $N=n \times n$. Assume that $M \ll N$, as usually is the case. Then the computer time required for calculating all the output samples is approximately

$$T_1 = Kn^2m^2 = kNM. \quad (88)$$

For $k \approx 30 \mu s$, $N = 200 \times 200$, and $M = 20 \times 20$, we have $T_1 = 8 \text{ min}$, which is a long time, considering the moderate sizes of input and filter samples.

The computer time can be cut down considerably, if the filter is separable, i.e., if

$$h_{ab} = h'_a h''_b. \quad (89)$$

Then (87) can be written as

$$p_{jk} = \sum_{a=0}^{m-1} \left\{ \sum_{b=0}^{m-1} g_{j-a,k-b} h''_b \right\} h'_a. \quad (90)$$

The inner summations can be evaluated first resulting in a computer time of

$$T'_1 = kn^2 2m = kn^2 2\sqrt{M}. \quad (91)$$

Observe that

$$T_1/T'_1 = m/2. \quad (92)$$

For $k \approx 30 \mu s$, $N = 200 \times 200$, and $M = 20 \times 20$, $T'_1 = T_1/10 \approx 0.8 \text{ min}$. Therefore, whenever situations permit, one should use a separable filter or a sum of a small number of them instead of a nonseparable filter.

An alternative way to do linear filtering is to work in the frequency domain [210]. We first take the Fourier transform of the input, and multiply it by the filter frequency response, and finally take

the inverse transform of this product to obtain the desired output. Assuming either $M \ll N$, or that the filter characteristic is given in the frequency domain, we observe that the computer time required in this method is approximately:

$$T_2 = k4N \log_2 N. \quad (93)$$

Comparison of (91), (94), and (96) yields:

$$T_2 < T_1, \quad \text{if } M > 4 \log_2 N \quad (94)$$

$$T_2 < T'_1, \quad \text{if } M > 4(\log_2 N)^2. \quad (95)$$

For example, for $N = 200 \times 200$: $T_2 < T_1$, if $M > 7 \times 7$; and $T_2 < T'_1$, if $M > 30 \times 30$.

Our discussions of nonrecursive filtering can be applied equally well to the calculation of correlation functions. We might mention in this respect that an improved algorithm for autocorrelation was recently proposed by Rader [173].

C. Two-Dimensional Nonrecursive Filters

Although a considerable amount of work has been done in the design of digital filters in one dimension, only very recently did researchers start to turn their attention to two-dimensional digital filters. In Subsections C and D, we shall discuss briefly some of the similarities and differences between one- and two-dimensional digital filters.

1) Sampling and Truncation: We are given an analog impulse response $h(x, y)$ where x and y are spatial variables. We would like to design a nonrecursive digital filter which approximates $h(x, y)$. Just like in the case of one dimension, there are two issues involved here, viz.: 1) How often do we have to sample? and 2) How shall we truncate $h(x, y)$? Both of these issues are resolved in the same way as in the one-dimensional case.

Let the Fourier transform of $h(x, y)$ be $H(u, v)$, and the Fourier transform of the input $f(x, y)$ be $F(u, v)$, where u and v are spatial frequencies. Assume

$$F(u, v) = 0 = H(u, v), \quad \text{for } (u^2 + v^2) > R^2 \quad (96)$$

where R is a constant. Then we should sample h and f with a period less than $1/R$ in both the x and the y direction. It is assumed that we use a square sampling grid.

To truncate $h(x, y)$, we multiply it by a window function $w(x, y)$:

$$w(x, y) = 0, \quad \text{for } |x| > X \text{ and } |y| > Y \quad (97)$$

where X and Y are positive constants. To reduce ringing in the frequency response, we should choose $w(x, y)$ such that its Fourier transform $W(u, v)$ has small sidelobes. Since many good windows have been discovered in one dimension [129], [37] we can use

$$w(x, y) = w_1(x)w_1(y) \quad (98)$$

where $w_1(x)$ is a good one-dimensional window. In some cases, we may want our two-dimensional window to be circularly symmetrical. Then, we can use [109]:

$$w(x, y) = w_1(\sqrt{x^2 + y^2}). \quad (99)$$

To actually carry out the nonrecursive filtering, we can either do a direct convolution, or use the FFT, just like in the one-dimensional case.

2) Circularly Symmetrical Filters: Suppose the given analog impulse response is circularly symmetrical, and we wish to approximate it by a nonrecursive digital filter which is as nearly circularly symmetrical as possible. The obvious thing to do would be to sample

$h(x, y)$ by a polar raster, i.e., to sample at the points with polar coordinates $(m\Delta\gamma, n\Delta\theta)$ where $\Delta\gamma$ and $\Delta\theta = 2\pi/N$ are constants, and $m=0, 1, 2, \dots; n=0, 1, 2, \dots, N-1$. However, we can do neither direct discrete convolution nor FFT conveniently with polar samples. Therefore, if we insist on a sampling raster which is more nearly circularly symmetrical than a square one, we should use a triangular raster. To do direct convolution and FFT on a triangular raster is completely analogous to doing them on a square raster.

D. Two-Dimensional Recursive Filters

1) *A Fundamental Curse*: A fundamental curse in two-dimensional recursive filtering is that the fundamental theorem of algebra in one dimension does not extend to two dimensions. In one dimension, any polynomial $P(Z)$ of degree n can be factored into n first-degree factors:

$$P(Z) = K(Z - Z_1)(Z - Z_2) \cdots (Z - Z_n) \quad (100)$$

where K and Z_i are constants. There is no corresponding factorization for a polynomial in two variables $P(Z_1, Z_2)$.

One implication of this curse is that we cannot realize our two-dimensional recursive filters in parallel or cascade form to reduce the effect of digitization errors.

Another implication of this curse is that the test of the stability of two-dimensional recursive filters is almost impossible except for very simple filters.

2) *Stability*: A basic stability theorem for two-dimensional recursive filters, due to Shanks [194], states that: A recursive filter with Z transform $H(Z_1, Z_2) = A(Z_1, Z_2)/B(Z_1, Z_2)$, where A and B are polynomials in Z_1 and Z_2 , is stable if and only if there are no values of Z_1 and Z_2 such that $|Z_1| \leq 1, |Z_2| \leq 1$, and $B(Z_1, Z_2) = 0$. By definition

$$\begin{cases} Z_1 = e^{-s_1 a} \\ Z_2 = e^{-s_2 b} \end{cases} \quad (101a)$$

$$(101b)$$

where s_1 and s_2 are, respectively, the horizontal and the vertical complex spatial frequencies, and a and b are constants (sampling periods in the horizontal and the vertical directions, respectively). It is not hard to convince oneself that to test stability using Shanks' theorem is hard work.

It can be shown [111] that after a suitable change of variables, Shanks' theorem becomes equivalent to a result in circuit theory due to Ansell [28], [225]. For filters with numerical coefficients, Ansell's stability-test procedure is often less tedious to use.

3) *Design Techniques*: The impulse-invariant technique [70] cannot be extended to two dimensions, since we cannot do partial-fraction expansion in two variables (thanks to our fundamental curse).

The method of moments [37] can be extended to two dimensions. So can a spatial-domain approximation technique of Shanks [193], [194], [50]. However, the filters designed according to these two methods may be unstable.

There is a class of one-dimensional methods, which we shall call transform methods, in which the analog transfer function $H_A(s)$ of a stable filter is given and an approximate digital filter $H_D(Z)$, is obtained by replacing s in H_A by $g(Z)$. The function g is suitably chosen so that stability is preserved. The transform method can be readily extended to two dimensions. Given $H_A(s_1, s_2)$, we get $H_D(Z_1, Z_2)$ by

$$H_D(Z_1, Z_2) = H_A(g(Z_1), g(Z_2)). \quad (102)$$

However, here the relation between $H_D(e^{-jw_a}, e^{-jv_b})$ and $H_A(ju, jv)$ is much harder to visualize than in the one-dimensional case. Also,

the specification of the filter is often given in the form of the magnitude of the frequency response. To obtain a stable $H_A(s_1, s_2)$ with $H_A(ju, jv)$ approximating the given magnitude response is much harder to do in two dimensions than in one dimension.

4) *Some Open Questions*: With respect to two-dimensional recursive filters, the most important practical questions we want to ask are as follows: 1) How do we design filters that are guaranteed to be stable? 2) If a given filter is unstable, how do we stabilize it without changing its frequency response?

One approach to attacking question 1) is to study what types of frequency responses we can get from classes of simple filters whose stability we know how to control.

With respect to question 2), we might mention a conjecture of Shanks [195]. Let $H(Z_1, Z_2) = 1/B(Z_1, Z_2)$ be an unstable filter. We first determine a least mean-square inverse of $B(Z_1, Z_2)$ which we call $G(Z_1, Z_2)$. We next determine a least mean-square inverse of $G(Z_1, Z_2)$, which we call $\hat{B}(Z_1, Z_2)$. Then Shanks' conjecture states that the filter $\hat{H}(Z_1, Z_2) = 1/\hat{B}(Z_1, Z_2)$ is stable and that the magnitude of the frequency response of \hat{H} is approximately equal to that of H . It was proven by Robinson [179] that a one-dimensional version of Shanks' procedure does yield stable (one-dimensional) filters. However, whether the procedure yields stable filters in two dimensions is still an open question. Also, no analysis is available on how close the magnitude of the frequency response of \hat{H} is to that of H .

We have yet another open question with respect to 2). In the one-dimensional case, if we are doing nonreal-time filtering, then we can always decompose an unstable filter with no poles on the unit circle into two stable ones recursing in opposite directions. We associate the poles of the original filter outside the unit circle with a filter recursing in the positive direction, and the poles inside the unit circle with a filter recursing in the negative direction. Is there an analogous procedure in two dimensions?

E. Separable-Sum Approximations

1) *The Main Result*: In this section, we present a result which finds applications in the design of both nonrecursive and recursive filters in two dimensions.

We shall solve the problem of representing arbitrary $h(i, j)$; $i=1, 2, \dots, l; j=1, 2, \dots, m$ by a separable sum

$$h_a(i, j) = \sum_{k=1}^n f_k(i) \cdot g_k(j).$$

The approximation is such that the error, defined by

$$\varepsilon = \sum_{i,j} |h_a(i, j) - h(i, j)|^2 \quad (103)$$

is as small as possible. The solution is as follows. Consider $h(i, j)$ as an l by m matrix H , and assume that $l < m$. Then H may be written as [137]:

$$H = \sum_{k=1}^l u_k v_{kT}. \quad (104)$$

(u_k and v_k are column matrices. v_{kT} being the transpose of v_k is a row matrix.) The vector v_k is a normalized eigenvector of

$$H_T H v_k = \mu_k v_k \quad (105)$$

and $\mu_k \geq 0$. The vectors u_k are defined by

$$u_k = H v_k. \quad (106)$$

We order the vectors by the rule

$$k_1 \geq k_2 \rightarrow \mu_{k_1} \geq \mu_{k_2}.$$

The best approximation is obtained by

$$H_a = \sum_{k=1}^n u_k v_{k\tau} \quad (107)$$

and the error associated with this approximation is

$$\varepsilon = \sum_{k=n+1}^l \mu_k. \quad (108)$$

This is proven by Tretiak [219]. A similar result was obtained by Treitel and Shanks [218].

2) *Application to Nonrecursive Filters:* We have now a procedure for approximating an arbitrary two-dimensional filter by a sum of separable filters. Equation (108) shows that the sum of separable filters can be made to be identical to the desired filter by including all the terms with nonzero eigenvalues.

Let us consider the computational effort required in the approximation. The direct evaluation requires $(l \times m)$ multiplications and additions for each output point. The approximation, however, requires $(l+m) \times n$ operations. In general, if all the terms must be included, this is equal to $(l^2 + l \times m)$ and it will be less efficient than the direct method. If, however, the required filter is approximated closely by only a few terms, a substantial saving may be achieved. Whether or not this is practical can easily be seen by examining the spectrum of eigenvalues of (105).

The procedure was applied to the filter given in Table I. The following are the eigenvalues for this matrix.

$$66.47 \quad 6.27 \quad 2.07 \quad 1.19.$$

Since only those four of the eigenvalues are nonzero, this matrix can be represented exactly by a sum of four separable filters. The magnitude of these eigenvalues are such that an approximation with error of 4.5 percent can be obtained if a two-term approximation is used.

3) *Application to Recursive Filters:* Equation (104) can be considered as a (very poor) substitute for a fundamental theorem of algebra in two dimensions. Given an analog two-dimensional impulse response $h(x, y)$, we can first sample and truncate it, and then expand in a separable sum, (104), or an approximation thereof, (107). Then we can design one-dimensional recursive filters for the components $f_k(i)$ and $g_k(j)$, using all the one-dimensional techniques we have in store. However, unless the number of terms n in (107) is small, the resulting recursive filter will probably not be very efficient, i.e., it will contain a large number of terms.

F. Numerical Solution of Linear Integral Equations

As we mentioned in Section II-E, the problem of restoring an image degraded by an LSV system is that of solving the linear integral equation (63). The brute-force way of doing it is to digitize both sides of (63), yielding a set of linear algebraic equations.

$$\begin{bmatrix} p_1 \\ p_2 \\ \vdots \\ p_m \end{bmatrix} = \begin{bmatrix} k_{11} & k_{12} & \cdots & k_{1n} \\ k_{21} & k_{22} & \cdots & k_{2n} \\ \vdots & \vdots & \ddots & \vdots \\ k_{m1} & k_{m2} & \cdots & k_{mn} \end{bmatrix} \begin{bmatrix} f_1 \\ f_2 \\ \vdots \\ f_n \end{bmatrix} \quad (109)$$

where p_i and f_j are samples of $p(x, y)$ and $f(x, \beta)$ respectively, and k_{ij} are, except for a positive scale factor, samples of $k(x, y; \alpha, \beta)$. If we make $m=n$, and if the determinant of $[k_{ij}]$ is nonzero, then in principle, we can solve (109) for the f_i 's.

The number of samples we have to take in digitizing (63) was discussed by Huang [107] and Granger [79]. In almost all practical

TABLE I
A SAMPLED FILTER ARRAY

0	0	0	1	1	1	1	0	0	0
0	0	1	1	1	1	1	1	0	0
0	1	1	1	1	1	1	1	1	0
1	1	1	1	1	1	1	1	1	1
1	1	1	1	1	1	1	1	1	1
1	1	1	1	1	1	1	1	1	1
1	1	1	1	1	1	1	1	1	1
0	1	1	1	1	1	1	1	1	0
0	0	1	1	1	1	1	1	0	0
0	0	0	1	1	1	1	0	0	0

cases, the number will be so large that the solution of (109) is simply out of the question. Even in the case when the number of equations ($m=n$) is small enough (a few hundreds, say), their solution is still very tricky because of the noise contained in the degraded image. Instead of solving the equations directly, iterative methods are often much more preferred [137]. Also, we might want to oversample p to obtain more equations than unknowns (i.e., to make $m > n$), and then try to find a least-square solution for the f_i 's [137].

G. Geometrical Operations

Geometrical operations are useful when we want to correct for geometrical distortions in images and when we want to perform rotation or scale change on images.

The general problem is as follows. The relation between the desired image $g(x, y)$ and the original image $f(x, y)$ is first specified:

$$g(x, y) = f(a(x, y), b(x, y)) \quad (110)$$

where a and b are functions of x and y . Then, we are given the samples $f(i\Delta x, j\Delta y)$; $i, j = 1, 2, \dots, N$ from $f(x, y)$, and asked to determine the samples $g(i\Delta x, j\Delta y)$; $i, j = 1, 2, \dots, N$ (where Δx and Δy are constants).

One approach to solving this problem is to use interpolation. From (110) we have

$$g(i\Delta x, j\Delta y) = f(a(i\Delta x, j\Delta y), b(i\Delta x, j\Delta y)). \quad (111)$$

Let I and J be two fixed integers, and let (a_0, b_0) , where $a_0 = a(I\Delta x, J\Delta y)$, $b_0 = b(I\Delta x, J\Delta y)$, lie in the rectangle with vertices $p_1 = (K\Delta x, L\Delta y)$, $p_2 = (K\Delta x, (L+1)\Delta y)$, $p_3 = ((K+1)\Delta x, L\Delta y)$ and $p_4 = ((K+1)\Delta x, (L+1)\Delta y)$. Let $a_0 = (K+\alpha)\Delta x$, and $b_0 = (L+\beta)\Delta y$. Then, using bilinear interpolation, we have

$$\begin{aligned} g(I\Delta x, J\Delta y) &= f(a_0, b_0) \\ &= f(p_1)(1 - \alpha)(1 - \beta) + f(p_2)(1 - \alpha)\beta \\ &\quad + f(p_3)\alpha(1 - \beta) + f(p_4)\alpha\beta. \end{aligned} \quad (112)$$

More elaborate procedures may be developed by using higher order polynomials for interpolating functions. For rotation and scale change, several simpler methods have been studied [124].

H. Some Nonlinear Operations

The flexibility of a digital computer permits it to perform many nonlinear operations required in image processing.

1) *Edge Extraction:* The gradient and the Laplacian operators are often used in extracting edges in an image. In the computer, these operators must be approximated by finite differences. Operators built of finite differences cannot be invariant under rotation, though they can be approximated arbitrarily closely. The squared gradient operator may be approximated by

$$|\nabla f|^2 \approx (f(i+1,j+1) - f(i,j))^2 + (f(i+1,j) - f(i,j+1))^2 \quad (113)$$

and the Laplacian by

$$\nabla^2 f \approx f(i+1,j) + f(i,j+1) + f(i-1,j) + f(i,j-1) - 4f(i,j). \quad (114)$$

These forms have a high degree of symmetry.

It is possible to transform differential operators to discrete operators by starting with the definition of a derivative given by

$$f_x \equiv f(i+1,j) - f(i,j) \quad (115a)$$

$$f_y \equiv f(i,j+1) - f(i,j) \quad (115b)$$

and to obtain higher order derivatives by applying this definition recursively. The operators obtained in this way tend to be not as symmetric as those defined earlier.

To extract edges, we set a threshold and call any point an edge point if the squared gradient (or the absolute value of the Laplacian) at that point exceeds the threshold.

2) *Contour Tracing*: In some efficient picture coding schemes, we want to trace contours in sampled two-level images. There are several ways of doing it. One of the simplest is due to Mason and Clemens [153]. Assume we have black objects in a white background. Then, the tracer simply turns right after a white point is encountered and left after a black point.

3) *Smoothing*: A sampled two-level image can be represented by a matrix of values f_{ij} ; $i, j = 1, 2, \dots$, where each f_{ij} is either 1 (black) or 0 (white). In such an image, we often have noise in the form of scattered black points in the white background and missing black points in the objects—the so-called pepper and salt noise. A popular way to reduce the noise is due to Dinneen [59].

The improved image g_{ij} is obtained from f_{ij} as follows. Let

$$S_{ij} = \sum_{p=-m}^m \sum_{q=-n}^n f_{i+p, j+q} \quad (116)$$

where m and n are fixed integers. Then

$$g_{ij} = \begin{cases} 1, & \text{if } S_{ij} \geq \theta \\ 0, & \text{if } S_{ij} < \theta \end{cases} \quad (117)$$

where θ is a fixed threshold.

4) *Thinning*: In transmitting line drawings, the thickness of the lines often contains little information. We might therefore want to "thin" each line to a one-sample wide line. To accomplish this, Sherman [198] proposed that we change a black point to white if in doing so we will neither create a gap nor shorten any one-sample wide line.

I. Comparison Between Coherent Optics and Digital Computer

1) *Flexibility*: Coherent optical systems are essentially limited to linear operations on the amplitude transmission variations of a film transparency. On the other hand, digital computers can be used to do linear operations on either the amplitude transmission, or the intensity transmission, or the density. More importantly, digital computers can also be used to do nonlinear operations.

2) *Capacity and Speed*: In a coherent optical system, the film is used as the storage, resulting in an enormous capacity. More importantly, the data on the film can be operated on in parallel, so that the speed is limited, in principle, only by the speed of light. Although a digital computer usually has a limited memory, any amount of auxiliary memory can be attached to it. If the computer has a film scanner, then films can also serve as its storage. However, present-day digital computers operate essentially sequentially on the data. Therefore, if a large number of data points need to be operated on, it takes a long time to bring the data into the central processor, and still a longer time to process them.

Let us consider an example. A giant coherent optical system [135] at the Institute of Science and Technology, University of Michigan, is capable of processing 70-mm films with a resolution of 100 cycles/mm. It can therefore do a Fourier transformation on approximately 2×10^8 data points essentially instantaneously.

Now suppose we do the same thing on a digital computer. It would take more than an hour just to read in the data points, if the computer film reader reads at $30 \mu\text{s}/\text{point}$. Assume that the Cooley and Tukey algorithm is used, and assume that the computer had a core memory of more than 4×10^8 words, it still would take about 100 h to perform the Fourier transform. (We assumed as before that it takes the computer $30 \mu\text{s}$ to do a basic operation.)

We might mention that several researchers have been developing computers which perform some parallel processing [69], [206]. These computers could be several orders of magnitude faster than the more conventional ones.

3) *Accuracy*: In digital processing, there are inherent errors due to sampling and amplitude quantization. These errors, however, can be made arbitrarily small by increasing the sampling rate and the number of quantization levels. In practice the accuracy of digital computer image processing is limited by the film scanner. It is probably difficult at present to build a film scanner with an accuracy better than 0.01 percent.

In a coherent optical system, there are various sources of errors, such as: imperfect optical components, film grain noise and nonlinearity, spurious thickness variations of film emulsions, errors in spatial filters, nonuniformity of light beam across the input aperture, and imperfect alignment of the optical system. These errors are not easy to control. One can probably expect an accuracy of only 3 to 5 percent in a coherent optical system. We might also mention the speckle effect [162] due to the coherence of the light which tends to obscure details in an image.

4) *Cost*: Coherent optical systems are usually cheaper than digital computers. However, large-aperture diffraction-limited coherent optical systems can be rather expensive. The giant system at the University of Michigan which we mentioned earlier cost about 500 000 dollars.

In summary, the main advantages of a coherent optical system are its information storage capacity and processing speed, and the main advantages of a digital computer are its flexibility and accuracy. Coherent optical systems are suitable for doing linear operations, such as Fourier transformation and linear filtering, on large-volume data; but when nonlinear operations or accurate linear operations on a limited amount of data are required, digital computers can be used to advantage. In some cases, although the filtering is best done by a coherent optical system, the spatial filter is most conveniently made on a digital computer.

VI. ELECTROOPTICAL DEVICES

A coherent optical system does linear operations in parallel, obtaining all output points at once, while most present-day digital computers do things serially. There are a number of special electro-optical devices which work partly in parallel and partly serially.

A. Linear Filtering by Analog Scanning

One can perform convolution by passing through the input transparency $f(\alpha, \beta)$ a light beam having an aperture function $h(x_0 - \alpha, y_0 - \beta)$, where x_0 and y_0 are constants. The output electrical signal of a phototube, which integrates the light beam after it has passed through the input transparency, will be the value of the desired output $g(x, y)$, at the point (x_0, y_0) . We can get as many output points as we like by scanning the beam across the input transparency.

The above scheme is of course limited to the case where $h(\alpha, \beta)$ is everywhere nonnegative. However, it can easily be modified to handle the more general case where $h(\alpha, \beta)$ can be negative as well.

as positive. For example, we can superimpose two light beams orthogonally polarized with respect to each other, the first one having an aperture function

$$h_1(\alpha, \beta) = \begin{cases} h(\alpha, \beta), & \text{when } h(\alpha, \beta) \geq 0 \\ 0, & \text{elsewhere} \end{cases} \quad (118a)$$

and the second one having an aperture function

$$h_2(\alpha, \beta) = \begin{cases} |h(\alpha, \beta)|, & \text{when } h(\alpha, \beta) < 0 \\ 0, & \text{elsewhere.} \end{cases} \quad (118b)$$

After the two beams have passed through the input transparency $f(\alpha, \beta)$ they can be picked up by two separate phototubes by using a beam splitter and two polarizers. The difference between the outputs of the two phototubes is the desired output $g(x, y)$.

Since noncoherent light can be used in this scheme we do not have the speckle and other noise problems associated with the case of the coherent light, where every little speck of dirt counts. The speed of this scheme is limited by the scanning speed.

A scanner along the lines discussed previously has been constructed by Shack [192], [213]. The same idea was used by Schreiber [188] in sharpening wire-photo pictures. Schreiber has also built a digital image recording-display CRT scanner which can be used to do some linear filtering. An example of using this scanner to do high-pass filtering on an X-ray picture is shown in Fig. 18. The reader will also be interested in the work of Craig [54] and Burnham [49].

B. Linear Filtering and Correlation by Image Tubes

Hawkins [95], [94] used a modified image storage tube to do linear filtering. The input light image $f(x, y)$ is first converted to an electron image, then by controlling the electric circuits associated with the tube, this image is deflected, amplified (or attenuated), and stored electrostatically on a mesh as $h_{ij}f(x - \alpha_i, y - \beta_j)$, where α_i , β_j , and h_{ij} are constants which can be either positive and negative. By superimposing many such images on the mesh, one can store

$$g_1(x, y) = \sum_{i,j} h_{ij}f(x - \alpha_i, y - \beta_j). \quad (119)$$

By choosing appropriate h_{ij} , α_i , and β_j , one can approximate $g(x, y)$, the desired output by $g_1(x, y)$ of (119). This image $g_1(x, y)$, which has been stored on the mesh, can be either converted to a proportional light image, or quantized electrically to yield a two-level display. The resolution of the tube is around 10 to 20 cycles (line pairs)/mm, and the total number of points is around 4×10^5 . A typical filtering operation takes a few milliseconds.

A slightly different type of image tube is available from ITT [118], [119] which can perform cross correlation between two consecutive input images. The first image f_1 is again stored electrostatically on a mesh. The operating potentials of the tube are then shifted electronically so that the photoelectrons from the photocathode, generated by the second input optical image f_2 , no longer strike the mesh but are allowed to partially penetrate or reflect from the mesh holes, depending on the stored charge pattern. The electron image passing through the mesh is then $f_1(\alpha, \beta)f_2(\alpha + x, \beta + y)$, where x and y are constants depending on the amount of deflection of the second image with respect to the first one. This electron image is integrated by an electron multiplier to give

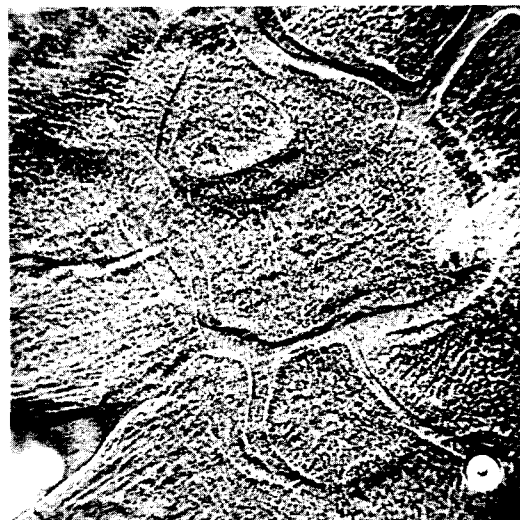
$$R_{12}(x, y) = \int_{-\infty}^{\infty} \int f_1(\alpha, \beta)f_2(\alpha + x, \beta + y) d\alpha d\beta \quad (120)$$

which is the cross-correlation function between f_1 and f_2 .

A different approach was taken by Abram *et al.* [24]. They modified an image dissector tube by replacing the conventional signal aperture by a 3×3 array of channeltron electron multipliers.



(a)



(b)

Fig. 18. X-ray picture. (a) Original. (b) High-pass filtered.

One then has access to nine points on the input image simultaneously and can operate on them electrically in parallel. In particular, we can take a weighted sum of the points to approximate linear filtering. Of course, for a good approximation, we need more points, i.e., a larger array of channeltron electron multipliers.

VII. IMAGE DESCRIPTION

In order to process an image on a digital computer, we have first to describe the image to the computer. In most cases, we feed the image into the computer in the form of a matrix, each element of which represents the brightness of an image sample point. This form of representation is quite appropriate for image enhancement work, since there we manipulate with a group of input sample values (e.g., doing linear filtering) to produce an output sample value. However, in pattern recognition and efficient picture coding, the matrix representation of an image is rather unnatural. Indeed, the goal of both pattern recognition and efficient picture coding is to find suitable ways of describing images. In pattern recognition, we want the description to be such that classification will be simplified. In the efficient coding of pictures, we want on the one hand to have a description of the image that is efficient and on the other hand to be able to reconstruct a good replica of the original image from the description.

The various methods of feature extraction in pattern recognition

and the several schemes of redundancy reduction in Section III can all be considered as ad hoc attempts of finding suitable ways of describing images. A fruitful direction of a unified study of image description seems to lie in the linguistic approach [19], [132], [100], [156], [82], [83], [130]. In this approach, we consider our images as generated from a set of basic elements according to a certain grammar. Although, up to the present, the linguistic approach has been applied successfully only to simple classes of images, such as line drawings, we have already seen its practical application to pattern recognition problems [60], [160], [141], [88].

We will not go into a detailed discussion of the linguistic approach to image description here. Rather, we would just like to mention in passing that one way of describing a continuous-tone image is to first decompose it into three components—edges, low-frequency part, and texture, as we proposed in Section III-D 5) and then use the linguistic approach to describe the edges and possibly Fourier spectra to describe the low-frequency part and the texture.

VIII. IMAGE QUALITY

The effects of various parameters on picture quality have been discussed by Schreiber [187b]. In most applications, picture quality is defined in subjective terms, and can only be measured in terms of observer response [168]. There is no good reason to suppose that subjective quality is a one-dimensional quantity, and if it is multi-dimensional, it cannot be ranked. In practice, it is treated as a scalar, and is defined in terms of the protocol used to measure it. It is usually specified in terms of a four-to-six step scale running from "excellent" to "unacceptable." A more attractive scale is graded in just-noticeable difference in image quality, so that subjective measurement of relevant system parameters is quite a difficult and tedious procedure. Measurement of subjective image quality is very difficult: one can see this by reflecting on the fact that a 30-percent increase in bandwidth produces a just-noticeable difference increment in appearance [32].

The practical problems in the measurement of subjective quality and the desire to design systems analytically brought forth several objective measures of subjective image quality. The most popular measures proposed to date are the mean-square error and its variants, such as the weighted mean-square error. These measures have the distinct advantage that they are mathematically tractable. They also appear to agree reasonably well with subjective evaluation in many cases.

A. Mean-Square Error Criteria

Let $f(x, y)$ be the input image, and $g(x, y)$ the output image where (x, y) are the spatial coordinates and f and g are brightness. We define the error as

$$\varepsilon(x, y) = f(x, y) - g(x, y) \quad (121)$$

and denote its Fourier transform by $E(u, v)$ where (u, v) are spatial frequencies. Then the mean-square error is

$$D_1(f, g) = \int_{-\infty}^{\infty} \int dx dy \varepsilon^2(x, y) = \int_{-\infty}^{\infty} \int du dv |E(u, v)|^2 \quad (122)$$

and the weighted mean-square error

$$D_2(f, g) = \int_{-\infty}^{\infty} \int du dv W(u, v) |E(u, v)|^2 \quad (123)$$

where $W(u, v)$ is called the weighting function. The weighting function reflects the sensitivity of the eye to various spatial frequency components in the image.

The mean-square error criteria have at least two defects. First, the subjective quality of a degraded image $g(x, y)$ depends not only on the error $\varepsilon(x, y)$ but also on the original image $f(x, y)$. Second, some image degradations are geometrical in nature—for example, block quantization using Hadamard transform (Section III-E) sometimes yields pictures containing "staircases" along the edges. The mean-square error criteria do not seem appropriate for geometrical distortions. A more satisfactory criterion should be based on some kind of edge error.

B. A Proposed Distortion Measure

We propose the distortion measure

$$D(f, g) = AD_a(f, g) + BD_b(f, g) \quad (124)$$

where A and B are positive constants, D_a is a weighted mean-square error modified to take care of the dependence on the original image, and D_b is a measure of edge error. One possible choice for D_a is

$$D_a(f, g) = \int_{-\infty}^{\infty} \int du dv |E(u, v)|^2 W_1(u, v) W_2(u, v) \quad (125)$$

where W_1 reflects the eye sensitivity, and W_2 reflects the dependence on the original image (and is a function of f). Much experimentation needs to be done to determine suitable forms for D_b and W_2 .

IX. CONCLUDING REMARKS

We have discussed in this paper some of the common problems underlying the three major areas of image processing, viz., image enhancement, efficient picture coding, and pattern recognition (with emphasis on the first two areas). In particular, we have described in some detail the mathematical operations we are most likely to encounter in image processing and ways of implementing these operations by optics and on digital computers. We have also sketched very briefly the problems of image description and image quality evaluation. These two latter topics are probably the most important among all image processing problems. The brevity of our description of them reflects the fact that much more work needs to be done.

BIBLIOGRAPHY

- [1] H. Andrews, *Computer Techniques in Image Processing*. New York: Academic Press, 1970.
- [2] *Appl Opt. (Special Issue on Optical Processing of Information)*, Apr. 1965.
- [3] G. Cheng *et al.*, Eds., *Pictorial Pattern Recognition*. Washington, D. C.: Thompson, 1968.
- [4] M. Faimen *et al.*, Eds., *Pertinent Concepts in Computer Graphics*. Urban, Ill.: Univ. Illinois Press, 1969.
- [5] G. L. Fisher *et al.*, Eds., *Optical Character Recognition*. Washington, D. C.: Spartan, 1962.
- [6] A. Grasselli, Ed., *Automatic Interpretation and Classification of Images*. New York: Academic Press, 1969.
- [7] T. S. Huang and O. J. Tretiak, Eds., *Picture Bandwidth Compression*. New York: Gordon & Breach, to be published in 1971.
- [8] *Proc. IEEE (Special Issue on Redundancy Reduction)*, vol. 55, Mar. 1967.
- [9] L. N. Kanal, Ed., *Pattern Recognition*. Washington, D. C.: Thompson, 1968.
- [10] P. A. Kokers and M. Eden, Eds., *Recognizing Patterns*. Cambridge, Mass.: M.I.T. Press, 1968.
- [11] B. Lipkin and A. Rosenfeld, Eds., *Picture Processing and Psychopictorics*. New York: Academic Press, 1970.
- [12] S. Morgan, Ed., "Restoration of atmospherically-degraded images," *NSF Summer Study Rep.*, Woods Hole, Mass., 1966.
- [13] M. Nagel, Ed., "Evaluation of motion-degraded images," in *Proc. NASA/ERC Seminar* (Cambridge, Mass., Dec. 1968).
- [14] G. Nagy, "State of the art in pattern recognition," *Proc. IEEE*, vol. 56, May 1968, pp. 836-862.
- [15] N. Y. Acad. Sci., *Proc. Conf. Data Extraction and Processing of Optical Images in the Medical and Biological Sciences* (New York, June 1967).
- [16] *Pattern Recognition J. (Special Issue on Image Enhancement)*, May 1970.

- [17] a) *Pattern Recognition J. (Special Issue on Character Recognition)*, Aug. 1970.
- b) *Pattern Recognition J. (Special Issue on Feature Extraction)*, Apr. 1971.
- [18] D. K. Pollock et al., Eds., *Optical Processing of Information*. Washington, D. C.: Spartan, 1963.
- [19] A. Rosenfeld, *Picture Processing by Computer*. New York: Academic Press, 1969.
- [20] *Proc. SPIE Seminar on Filmed Data and Computers* (Boston, Mass., June 1966).
- [21] *Proc. SPIE Seminar on Computerized Imaging Techniques* (Washington, D. C., June 1967).
- [22] J. T. Tippett et al., Eds., *Optical and Electro-Optical Information Processing*. Cambridge, Mass.: M.I.T. Press, 1965.
- [23] J. Tou, Ed., *Advances in Information Systems Science*, vol. 3. New York: Plenum, 1970.

REFERENCES

- [24] J. M. Abram, C. E. Catchpole, and G. W. Goodrich, "Image processing with a multiaperture image dissector," *SPIE J.*, vol. 6, 1968, pp. 93-96.
- [25] N. G. Altman, "Use of electro-optical image correlation for measuring and providing compensation for image motion," *op. cit.* [13].
- [26] G. B. Anderson and T. S. Huang, "Picture bandwidth compression by piecewise Fourier transformation," in *Proc. Purdue Centennial Symp. Information Processing* (Purdue Univ., Lafayette, Ind., Apr. 1969); also (revised version), "Piecewise Fourier transformation for picture bandwidth compression," *IEEE Trans. Commun. Technol.*, vol. COM-19, Apr. 1971, pp. 133-140.
- [27] H. C. Andrews, "Bibliography on rate distortion theory," *IEEE Trans. Inform. Theory (Corresp.)*, vol. IT-17, Mar. 1971, pp. 198-199.
- [28] H. G. Ansell, "On certain two-variable generalizations of circuit theory, with applications to networks of transmission lines and lumped reactances," *IEEE Trans. Circuit Theory*, vol. CT-11, June 1964, pp. 214-223.
- [29] M. Arm, M. King, A. Aimette, and B. Lambert, *Proc. Symp. Modern Optics*. Brooklyn, N. Y.: Polytechnic Press, 1967.
- [30] A. E. Attard and D. E. Brown, "Photoelectroplating light modulator," *Appl. Opt.*, vol. 7, Mar. 1968, pp. 511-515.
- [31] T. Baer, "Picture coding using the medial axis transform," S.M. thesis, Dep. Elec. Eng., Mass. Inst. Tech., Cambridge, May 1969.
- [32] M. W. Baldwin, Jr., "The subjective sharpness of simulated television images," *Bell Syst. Tech. J.*, vol. 19, Oct. 1940, pp. 563-568.
- [33] R. Barakat, "Numerical results concerning the transfer functions and total illuminance for optimum balanced 5th-order spherical aberration," *J. Opt. Soc. Amer.*, vol. 54, Jan. 1964, pp. 38-44.
- [34] C. W. Barnes, "Object restoration in a diffraction-limited imaging system," *J. Opt. Soc. Amer.*, vol. 56, May 1966, pp. 575-578.
- [35] M. A. Berkovitz, "Edge gradient analysis OTF accuracy study," in *Proc. SPIE Seminar on Modulation Transfer Function* (Boston, Mass., Mar. 1968).
- [36] F. C. Billingsley, "Applications of digital image processing," *Appl. Opt.*, vol. 9, Feb. 1970, pp. 289-299.
- [37] R. B. Blackman, *Linear Data-Smoothing and Prediction in Theory and Practice*. Reading, Mass.: Addison-Wesley, 1965.
- [38] E. S. Blackman, "Effects of noise on the determination of photographic system modulation transfer function," *Photogr. Sci. Eng.*, vol. 12, Sept.-Oct. 1968, pp. 244-250.
- [39] —, "Recovery of system transfer functions from noisy photographic records," in *Proc. SPIE Seminar on Image Information Recovery* (Philadelphia, Pa., 1969).
- [40] A. G. Bose, "A theory of nonlinear systems," MIT/RLE, Tech. Rep. 309, May 1956.
- [41] R. N. Bracewell, *The Fourier Transform and its Applications*. New York: McGraw-Hill, 1965.
- [42] C. P. C. Bray, "Comparative analysis of geometric vs diffraction heterochromatic lens evaluations using optical transfer function theory," *J. Opt. Soc. Amer.*, vol. 55, Sept. 1965, pp. 1136-1138.
- [43] G. C. Brock, *Physical Aspects of Aerial Photography*. New York: Dover, 1967.
- [44] K. Bromley, M. A. Monahan, J. F. Bryant, and B. J. Thompson, "Holographic subtraction," *Appl. Opt.*, vol. 10, Jan. 1971, pp. 174-180.
- [45] B. R. Brown and A. W. Lohmann, "Complex spatial filter with binary mask," *Appl. Opt.*, vol. 4, 1966, p. 967.
- [46] E. B. Brown, "Prediction and compensation of linear image motions in aerial cameras," *op. cit.* [13].
- [47] O. Bryngdahl and A. Lohmann, "Holographic penetration of turbulence," *op. cit.* [13].
- [48] G. J. Buck and J. J. Gustincic, "Resolution limitations of a finite aperture," *IEEE Trans. Antennas Propagat.*, vol. AP-15, May 1967, pp. 376-381.
- [49] D. C. Burnham, "Electronic averaging of one-dimensional television pictures," *Appl. Opt.*, vol. 9, Nov. 1970, pp. 2565-2568.
- [50] C. S. Burrus and T. W. Parks, "Time domain design of recursive digital filters," *IEEE Trans. Audio Electroacoust.*, vol. AU-18, June 1970, pp. 137-141.
- [51] J. C. Cassidy, "Magneto-optically generated inputs in optical data processing," *J. Opt. Soc. Amer.*, vol. 61, Mar. 1971, pp. 378-385.
- [52] a) D. A. Chesler, "Resolution enhancement by variable filtering," *Phys. Res. Lab.*, Massachusetts General Hospital, Boston, Internal Rep., Jan. 1969.
b) P. S. Considine, R. H. Dumais, and R. A. Profio, "Interactive optical enhancement devices," presented at the SPIE Seminar on Recent Advances in the Evaluation of the Photographic Image, Boston, Mass., July 1971.
- [53] J. W. Cooley and J. W. Tukey, "An algorithm for the machine calculation of complex Fourier series," *Math. Comput.*, vol. 19, 1965, pp. 297-301.
- [54] D. R. Craig, in *Proc. SPIE Seminar on Image Enhancement* (St. Louis, Mo., Mar. 1963).
- [55] L. J. Cutrona, "Recent developments in coherent optical technology," *op. cit.* [22].
- [56] L. J. Cutrona, E. N. Leith, C. J. Palermo, and L. J. Porcello, "Optical data processing and filtering systems," *IRE Trans. Inform. Theory*, vol. IT-6, June 1960, pp. 386-400.
- [57] L. D. Davission, "Data compression: Theory and application," in *Proc. Kelly Communications Conf.* (Univ. Missouri, Rolla, Oct. 1970).
- [58] D. J. De Rosier and A. Klug, "Reconstruction of three-dimensional structures from electron micrographs," *Nature*, vol. 217, Jan. 13, 1968, pp. 130-134.
- [59] G. P. Dinneen, "Programming pattern recognition" in *1955 Proc. Western Joint Computer Conf.* (Los Angeles, Calif.), vol. 7, pp. 91-100.
- [60] M. Eden, "Handwriting generation and recognition," *IRE Trans. Inform. Theory*, vol. IT-8, Feb. 1962, pp. 160-166.
- [61] D. G. Falconer, "Image enhancement and film-grain noise," *Opt. Acta*, vol. 17, Sept. 1970, pp. 693-705.
- [62] A. E. Filip, "Estimation of the impulse response of image-degrading systems," *MIT/RLE Quart. Progr. Rep.* 99, Oct. 15, 1970, pp. 135-140.
- [63] C. Flammer, *Spheroidal Wave Functions*. Stanford, Calif.: Stanford Univ. Press, 1957.
- [64] D. L. Fried, "Optical resolution through a randomly inhomogeneous medium for very long and very short exposures," *J. Opt. Soc. Amer.*, vol. 56, Oct. 1966, pp. 1372-1379.
- [65] —, "Limiting resolution looking down through the atmosphere," *J. Opt. Soc. Amer.*, vol. 56, Oct. 1966, pp. 1380-1384.
- [66] B. R. Frieden, "Bandlimited reconstruction of optical objects and spectra," *J. Opt. Soc. Amer.*, vol. 57, Aug. 1967, pp. 1013-1019.
- [67] —, "Optimum nonlinear processing of noisy images," *J. Opt. Soc. Amer.*, vol. 58, Sept. 1968.
- [68] H. Frieser, *Photogr. Sci. Eng.*, vol. 4, 1960, p. 324.
- [69] B. Gold, I. L. Lebow, P. G. McHugh, and C. M. Rader, "The FDP, a fast programmable signal processor," *IEEE Trans. Comput.*, vol. C-20, Jan. 1971, pp. 33-38.
- [70] B. Gold and C. M. Rader, *Digital Processing of Signals*. New York: McGraw-Hill, 1969.
- [71] I. J. Good, *J. Roy. Statist. Soc.*, vol. B20, 1958, pp. 361-372; also, Addendum, vol. B22, 1960, pp. 372-375.
- [72] —, "The relationship between two fast Fourier transforms," *IEEE Trans. Comput. (Short Notes)*, vol. C-20, Mar. 1971, pp. 310-317.
- [73] J. W. Goodman, "Use of a large-aperture optical system as a triple interferometer for removal of atmospheric image degradations," *op. cit.* [13].
- [74] —, *Introduction to Fourier Optics*. New York: McGraw-Hill, 1968.
- [75] J. W. Goodman, D. W. Jackson, M. Lehmann, and J. W. Knotts, "Holographic imagery through atmospheric inhomogeneities," *op. cit.* [13].
- [76] J. W. Goodman and W. T. Rhodes, "An optical system designed for image processing," *op. cit.* [16].
- [77] D. N. Graham, "Image transmission by two-dimensional contour coding," *Proc. IEEE*, vol. 55, Mar. 1967, pp. 336-346.
- [78] R. E. Graham, "Snow removal—A noise-stripping process for picture signals," *IRE Trans. Inform. Theory*, vol. IT-8, Feb. 1962, pp. 129-144.
- [79] E. M. Granger, "Restoration of images degraded by spatially-varying smear," *op. cit.* [13].
- [80] R. L. Green, "Diffraction in lensless correlation," *Appl. Opt.*, vol. 7, 1968, pp. 1237-1239.
- [81] R. L. Gregory, "A technique for minimizing the effects of atmospheric disturbance on photographic telescopes," *Nature*, vol. 203, July 18, 1964, pp. 274-275.
- [82] U. Grenander, "Foundations of pattern analysis," *Quart. Appl. Math.*, vol. 27, Apr. 1969, pp. 1-55.
- [83] —, "A unified theory of patterns," in *Advances in Computers*. New York: Academic Press, 1969.
- [84] E. A. Guillemin, *Synthesis of Passive Networks*. New York: Wiley, 1957.
- [85] A. Habibi and P. A. Wintz, "Image coding by linear transformations and block quantization," *IEEE Trans. Commun. Technol.*, vol. COM-19, Feb. 1971, pp. 50-62.

- [86] H. J. Hall and H. K. Howell, Eds., *Photographic Considerations for Aerospace*. Lexington, Mass.: Itek Corp., 1965.
- [87] H. B. Hammill and C. Holladay, "The effects of certain approximations in image quality evaluation from edge traces," *SPIE J.*, vol. 8, Aug.-Sept. 1970, pp. 223-228.
- [88] W. J. Hankley and J. T. Tou, "Automatic fingerprint interpretation and classification via contextual analysis and topological coding," *op. cit.* [3].
- [89] J. Harris, "Restoration of atmospherically distorted images," Scripps Inst. Oceanography, Univ. California, San Diego, SIO Ref. 63-10, Mar. 1963.
- [90] J. L. Harris, "Diffraction and resolving power," *J. Opt. Soc. Amer.*, vol. 54, July 1964, pp. 931-936.
- [91] —, "Image evaluation and restoration," *J. Opt. Soc. Amer.*, vol. 56, May 1966, pp. 569-574.
- [92] —, "Potential and limitations of techniques for processing linear motion-degraded imagery," *op. cit.* [13].
- [93] —, "Information extraction from diffraction limited imagery," *Pattern Recognition J.*, vol. 2, May 1970, pp. 69-77.
- [94] J. K. Hawkins, "Parallel electro-optical picture processing," *op. cit.* [3].
- [95] J. K. Hawkins and C. J. Munsey, "Image processing by electron-optical techniques," *J. Opt. Soc. Amer.*, vol. 57, July 1967, pp. 914-918.
- [96] R. A. Heinz, J. O. Artman, and S. H. Lee, "Matrix multiplication by optical methods," *Appl. Opt.*, vol. 9, Sept. 1970, pp. 2161-2168.
- [97] C. W. Helstrom, "Image restoration by the method of least squares," *J. Opt. Soc. Amer.*, vol. 57, Mar. 1967, pp. 297-303.
- [98] L. O. Hendeberg and W. E. Welander, "Experimental transfer characteristics of image motion and air conditions in aerial photography," *Appl. Opt.*, vol. 2, 1963, pp. 379-386.
- [99] S. Herman, *Proc. Symp. Modern Optics*. Brooklyn, N. Y.: Polytechnic Press, 1967.
- [100] Y. C. Ho and A. K. Agrawala, "On pattern classification algorithms: Introduction and survey," *Proc. IEEE*, vol. 56, Dec. 1968, pp. 2101-2114.
- [101] H. H. Hopkins, "The frequency response of a defocused optical system," *Proc. Roy. Soc., Ser. A*, vol. 231, 1955, pp. 91-103.
- [102] —, "Interferometric methods for the study of diffraction images," *Opt. Acta*, vol. 2, Apr. 1955, pp. 23-29.
- [103] J. L. Horner, "Optical spatial filtering with the least mean-square-error filter," *J. Opt. Soc. Amer.*, vol. 59, May 1969, pp. 553-558.
- [104] —, "Optical restoration of images blurred by atmospheric turbulence using optimum filter theory," *Appl. Opt.*, vol. 9, Jan. 1970, pp. 167-171.
- [105] J. Y. Huang and P. M. Schultheiss, "Block quantization of correlated Gaussian random variables," *IEEE Trans. Commun. Syst.*, vol. CS-11, Sept. 1963, pp. 289-296.
- [106] T. S. Huang, "Some notes on film grain noise," *op. cit.* [12].
- [107] —, "Digital analysis of linear shift-variant systems," *op. cit.* [13].
- [108] —, "Coding of graphical data," EG&G Tech. Rep. B-3742, Mar. 1968.
- [109] —, "Two-dimensional windows," M.I.T. Lincoln Lab. Tech. Note 1970-41, Dec. 31, 1970.
- [110] —, "How the fast Fourier transform got its name," *Comput.*, May 1971.
- [111] —, "Stability of two-dimensional recursive filters," M.I.T. Lincoln Lab. Tech. Note 1971-20, May 19, 1971.
- [112] T. S. Huang and O. J. Tretiak, "Research in picture processing," *op. cit.* [22].
- [113] —, "A pseudorandom multiplex system for facsimile transmission," *IEEE Trans. Commun. Technol.*, vol. COM-16, June 1968, pp. 436-438.
- [114] T. S. Huang and J. W. Woods, "Picture bandwidth compression by block quantization," presented at the Int. Symp. Information Theory, Ellenville, N. Y., Jan. 1969; abstract in *IEEE Trans. Inform. Theory*, vol. IT-16, Jan. 1970, p. 119.
- [115] D. A. Huffman, "A method for the construction of minimum-redundancy codes," *Proc. IRE*, vol. 40, Sept. 1952, pp. 1098-1101.
- [116] R. E. Hufnagel, "An improved model turbulent atmosphere," *op. cit.* [12, vol. 2].
- [117] R. E. Hufnagel and N. R. Stanley, "Modulation transfer function associated with image transmission through turbulent media," *J. Opt. Soc. Amer.*, vol. 54, Jan. 1964, pp. 52-61.
- [118] ITT Industrial Laboratories, "Pattern recognition image tubes," Application Note E13, Feb. 1967.
- [119] —, "Seesaw image correlation tubes," *News Lett.*, June 1967.
- [120] P. A. Jansson, "Method for determining the response function of a high-resolution infrared spectrometer," *J. Opt. Soc. Amer.*, vol. 60, Feb. 1970, pp. 184-191.
- [121] P. A. Jansson, R. H. Hunt, and E. K. Plyler, "Response function for spectral resolution enhancement," *J. Opt. Soc. Amer.*, vol. 58, Dec. 1968, pp. 1665-1666.
- [122] —, "Resolution enhancement of spectra," *J. Opt. Soc. Amer.*, vol. 60, May 1970, pp. 596-599.
- [123] N. Jensen, *Optical and Photographic Reconnaissance Systems*. New York: Wiley, 1968.
- [124] E. G. Johnston and A. Rosenfeld, "Geometrical operations on digitized pictures," *op. cit.* [11].
- [125] R. A. Jones, "An automated technique for deriving MTF's from edge traces," *Photogr. Sci. Engr.*, vol. 11, Mar.-Apr. 1967, pp. 102-106.
- [126] —, "Accuracy test procedure for image evaluation techniques," *Appl. Opt.*, vol. 7, Jan. 1968, pp. 133-136.
- [127] R. A. Jones and E. C. Yeadon, "Determination of the spread function from noisy edge scans," *Photogr. Sci. Engr.*, vol. 13, July-Aug. 1969, pp. 200-204.
- [128] R. J. Jones, "V/h sensor theory and performance," *op. cit.* [13].
- [129] J. F. Kaiser, "Digital filters," in *System Analysis by Digital Computer*, F. F. Kuo and J. F. Kaiser, Eds. New York: Wiley, 1966, ch. 7.
- [130] S. Kaneff, Ed., *Picture Language Machine*. New York: Academic Press, 1970.
- [131] R. S. Kennedy, "On statistical estimation of incoherently illuminated objects," *op. cit.* [12, vol. 2].
- [132] R. A. Kirsch, "Computer interpretation of English text and picture patterns," *IEEE Trans. Electron. Comput.*, vol. EC-13, Aug. 1964, pp. 363-376.
- [133] A. N. Kolmogorov, "On the Shannon theory of information transmission in the case of continuous signals," *IRE Trans. Inform. Theory*, vol. IT-2, Dec. 1956, pp. 102-108.
- [134] V. A. Kovalsky, "Pattern recognition: Heuristics or science?" *op. cit.* [23].
- [135] A. Kozma and N. Massay, *1964 Annual Radar Symp.* (Inst. Sci. Technol., Univ. Michigan, Ann Arbor).
- [136] H. P. Kramer and M. W. Mathews, "A linear coding for transmitting a set of correlated signals," *IRE Trans. Inform. Theory*, vol. IT-2, Sept. 1956, pp. 41-46.
- [137] C. Lanczos, *Linear Differential Operators*. Princeton, N. J.: Van Nostrand, 1961, pp. 115-118.
- [138] H. J. Landau and H. O. Pollak, "Prolate spheroidal wave functions, Fourier analysis, and uncertainty—II," *Bell Syst. Tech. J.*, vol. 40, 1961, pp. 65-84.
- [139] —, "Prolate spheroidal wave functions, Fourier analysis and uncertainty—IV: The dimension of the space of essentially time- and band-limited signals," *Bell Syst. Tech. J.*, July 1962.
- [140] H. J. Landau and D. Slepian, "Some computer experiments in picture processing for bandwidth reduction," *Bell Syst. Tech. J.*, 1970.
- [141] R. S. Ledley, L. S. Rotolo, J. B. Wilson, M. Nelson, T. J. Golab, and J. Jacobsen, "Pattern recognition studies in the biomedical sciences," in *1966 Spring Joint Computer Conf., AFIPS Conf. Proc.* (Boston, Mass.).
- [142] W. H. Lee, "Computer generation of holograms and spatial filters," Sc.D. dissertation, Dep. Elec. Eng., Mass. Inst. Tech., Cambridge, Sept. 1969.
- [143] —, "Sampled Fourier transform hologram generated by computer," *Appl. Opt.*, vol. 9, Mar. 1970, pp. 639-643.
- [144] —, "Filter design for optical data processors," *op. cit.* [16].
- [145] L. Levi, "Motion blurring with decaying defector response," *Appl. Opt.*, vol. 10, Jan. 1971, pp. 38-41.
- [146] M. D. Levine, "Feature extraction: A survey," *Proc. IEEE*, vol. 57, Aug. 1969, pp. 1391-1407.
- [147] A. Lohmann, "Aktive Kontrastübertragungstheorie," *Opt. Acta*, vol. 6, Oct. 1959, pp. 319-338.
- [148] A. W. Lohmann and D. P. Paris, "Space-variant image formation," *J. Opt. Soc. Amer.*, vol. 55, Aug. 1965, pp. 1007-1013.
- [149] —, "Fresnel hologram generated by computer," *Appl. Opt.*, vol. 6, 1968, p. 1739.
- [150] R. F. Lutomirski and H. T. Yura, "Modulation-transfer function and phase-structure function of an optical wave in a turbulent medium—I," *J. Opt. Soc. Amer.*, vol. 59, Aug. 1969, pp. 999-1000.
- [151] D. P. MacAdam, "Digital image restoration by constrained deconvolution," *J. Opt. Soc. Amer.*, vol. 60, Dec. 1970, pp. 1617-1627.
- [152] A. S. Marathay, "Realization of complex spatial filters with polarized light," *J. Opt. Soc. Amer.*, vol. 59, June 1969, pp. 748-752.
- [153] S. J. Mason and J. K. Clemens, "Character recognition in an experimental reading machine for the blind," *op. cit.* [10].
- [154] M. J. Mazurowski and R. E. Kinzly, "The precision of edge analysis applied to the evaluation of motion-degraded images," *op. cit.* [13].
- [155] W. Meyer-Eppeler and G. Darius, *Proc. 3rd London Symp. Information Theory*, C. Cherry, Ed. New York: Academic Press, 1956.
- [156] W. F. Miller and A. C. Shaw, "Linguistic methods in picture processing—A survey," in *1968 Fall Joint Computer Conf., AFIPS Conf. Proc.*, pp. 279-290.
- [157] J. Minkoff, W. R. Bennett, L. B. Lambert, M. Arm, and S. Bernstein, *Proc. Symp. Modern Optics*. Brooklyn, N. Y.: Polytechnic Press, 1967.
- [158] L. Miyamoto, "Wave optics and geometrical optics in optical design," in *Progress in Optics*, vol. 1, E. Wolf, Ed. Amsterdam, The Netherlands: North-Holland, 1961.
- [159] J. C. Moldon, "High resolution image estimation in a turbulent environment," *op. cit.* [16].
- [160] R. Narasimhan, "Labelling schemata and syntactic description of pictures," *Inform. Contr.*, vol. 7, 1964.
- [161] R. Nathan, "Picture enhancement for the moon, Mars, and man," *op. cit.* [3].
- [162] B. M. Oliver, "Sparkling spots and random diffraction," *Proc. IEEE*

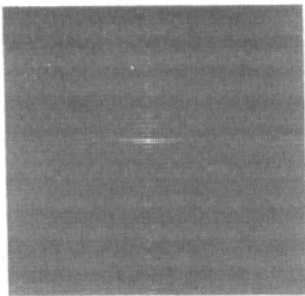
- (Corresp.), vol. 51, Jan. 1963, pp. 220-221.
- [163] B. M. Oliver, J. R. Pierce, and C. E. Shannon, "The philosophy of PCM," *Proc. IRE*, vol. 36, Nov. 1948, pp. 1324-1331.
- [164] E. L. O'Neill, *Introduction to Statistical Optics*. Reading, Mass.: Addison-Wesley, 1963.
- [165] A. V. Oppenheim, R. W. Schafer, and T. G. Stockham, Jr., "Nonlinear filtering of multiplied and convolved signals," *Proc. IEEE*, vol. 56, Aug. 1968, pp. 1264-1291.
- [166] D. P. Paris, "Influence of image motion on the resolution of a photographic system—I," *Photogr. Sci. Eng.*, vol. 6, 1962, pp. 55-59.
- [167] —, "Influence of image motion on the resolution of a photographic system—II," *Photogr. Sci. Eng.*, vol. 7, 1963, pp. 233-236.
- [168] D. E. Pearson, "Techniques for scaling television picture quality," *op. cit.* [7].
- [169] D. P. Peterson and D. Middleton, "Sampling and reconstruction of wave-number-limited functions in n -dimensional Euclidean spaces," *Inform. Contr.*, vol. 5, 1962, pp. 279-323.
- [170] S. M. Pizer and H. G. Vetter, "Processing quantum limited images," *op. cit.* [11].
- [171] W. J. Popplebaum, "Adaptive on-line Fourier transform," *op. cit.* [3].
- [172] W. K. Pratt, J. Kane, and H. G. Andrews, "Hadamard transform image coding," *Proc. IEEE*, vol. 57, Jan. 1969, pp. 58-68.
- [173] C. M. Rader, "An improved algorithm for high speed autocorrelation with applications to spectral estimation," *IEEE Trans. Audio Electro-acoust.*, vol. AU-18, Dec. 1970, pp. 439-441.
- [174] W. R. Crowther and C. M. Rader, "Efficient coding of vocoder channel signals using linear transformation," *Proc. IEEE (Lett.)*, vol. 54, Nov. 1966, pp. 1594-1595.
- [175] C. L. Rino, "Bandlimited image restoration by linear mean-square estimation," *J. Opt. Soc. Amer.*, vol. 59, May 1969, pp. 547-553.
- [176] —, "The application of prolate spheroidal wave functions to the detection and estimation of band-limited signals," *Proc. IEEE (Lett.)*, vol. 58, Feb. 1970, pp. 248-249.
- [177] G. M. Robbins, "Impulse response of a lens with Seidel aberrations," *MIT/RLE Quart. Progr. Rep.* 93, Apr. 5, 1969, pp. 243-250.
- [178] —, "The inversion of linear shift-variant imaging systems," Sc.D. dissertation, Dep. Elec. Eng., Mass. Inst. Tech., Cambridge, Aug. 1970.
- [179] E. A. Robinson, *Statistical Communication and Detection*. New York: Hafner, 1967.
- [180] P. G. Roetling, R. C. Haas, and R. E. Kinzly, "Some practical aspects of measurement and restoration of motion-degraded images," *op. cit.* [13].
- [181] C. K. Rushforth and R. W. Harris, "Restoration resolution, and noise," *J. Opt. Soc. Amer.*, vol. 58, Apr. 1968, pp. 539-545.
- [182] J. B. Rust, *Opt. Spectra*, vol. 2, 1968, p. 41.
- [183] D. Sakrison, "The rate distortion function of a Gaussian process with a weighted square error criterion," *IEEE Trans. Inform. Theory*, vol. IT-14, May 1968, pp. 506-508.
- [184] —, "The rate distortion function for a class of sources," *Inform. Contr.*, vol. 15, Aug. 1969, pp. 165-195.
- [185] —, "Factors involved in applying rate-distortion theory to image transmission," in *Proc. Kelly Communications Conf.* (Univ. Missouri, Rolla, Oct. 1970).
- [186] K. Sayanagi, *J. Appl. Phys. (Japan)*, vol. 27, no. 10, 1958, pp. 623, 632.
- [187] a) W. F. Schreiber, "The mathematical foundation of the synthetic highs system," *MIT/RLE Quart. Progr. Rep.* 68, Jan. 1963, p. 149.
b) —, "Picture coding," *op. cit.* [8, pp. 320-330].
- [188] —, "Wirephoto quality improvement by unsharp masking," *op. cit.* [16].
- [189] W. F. Schreiber, T. S. Huang, and O. J. Tretiak, "Contour coding of images," *WESCON Conv. Rec.*, Aug. 1968.
- [190] R. M. Scott, *Photogr. Sci. Eng.*, vol. 3, 1959, p. 201.
- [191] R. V. Shack, "The influence of image motion and shutter operation on the photographic transfer function," *Appl. Opt.*, vol. 3, Oct. 1964, pp. 1171-1181.
- [192] —, "Image processing by an optical analog device," *op. cit.* [16].
- [193] J. L. Shanks, "Recursion filters for digital processing," *Geophys.*, vol. 33, Feb. 1967, pp. 33-51.
- [194] —, "Two-dimensional recursive filters," *SWIECO Rec.*, 1969, pp. 19E1-19E8.
- [195] —, "The design of stable two-dimensional recursive filters," in *Proc. Kelly Communications Conf.* (Univ. Missouri, Rolla, Oct. 1970).
- [196] C. E. Shannon and W. Weaver, *The Mathematical Theory of Communications*. Urbana, Ill.: Univ. Illinois Press, 1949.
- [197] C. B. Shaw, "Improvement of the resolution of an instrument by numerical solution of an integral equation," *Autonetics*, Anaheim, Calif., Autonetics Rep. X70-510/501, Mar. 27, 1970.
- [198] H. Sherman, "A quasi-topological method for the recognition of line patterns," in *Proc. Int. Conf. Information Processing* (Paris, UNESCO, June 1959), pp. 232-238.
- [199] A. R. Shulman, *Optical Data Processing*. New York: Wiley, 1970.
- [200] D. Slepian, "Prolate spheroidal wave functions, Fourier analysis, and uncertainty—IV: Extensions to many dimensions; generalized prolate spheroidal functions," *Bell Syst. Tech. J.*, Nov. 1964.
- [201] —, "Some asymptotic expansions for prolate spheroidal wave functions," *J. Math. Phys.*, vol. 44, June 1965, pp. 99-140.
- [202] —, "Linear least-squares filtering of distorted images," *J. Opt. Soc. Amer.*, vol. 57, July 1967, pp. 918-922.
- [203] —, "Restoration of photographs blurred by image motion," *Bell Syst. Tech. J.*, vol. 46, Dec. 1967, pp. 2353-2362.
- [204] D. Slepian and H. O. Pollak, "Prolate spheroidal wave functions, Fourier analysis and uncertainty—I," *Bell Syst. Tech. J.*, vol. 40, 1961, pp. 43-46.
- [205] D. Slepian and E. Sonnenblick, "Eigenvalues associated with prolate spheroidal wave functions of zero order," *Bell Syst. Tech. J.*, Oct. 1965.
- [206] D. L. Slotnick, "The fastest computer," *Sci. Amer.*, vol. 224, Feb. 1971, pp. 76-87.
- [207] a) H. A. Smith, "Improvement of the resolution of a linear scanning device," *SIAM J. Appl. Math.*, vol. 14, Jan. 1966, pp. 23-40.
b) S. C. Som, "Analysis of the effect of linear smear on photographic images," *J. Opt. Soc. Amer.*, vol. 61, July 1971, pp. 859-864.
- [208] D. R. Spencer and T. S. Huang, "Bit-plane encoding of continuous-tone pictures," in *Proc. Symp. Computer Processing in Communications*. Brooklyn, N. Y.: Polytechnic Press, 1969.
- [209] *Proc. SPIE Seminar on Modulation Transfer Function* (Boston, Mass., Mar. 1968).
- [210] T. G. Stockham, Jr., in *1966 Spring Joint Computer Conf., AFIPS Conf. Proc.*, vol. 28.
- [211] P. A. Stokseth, "Properties of a defocused optical system," *J. Opt. Soc. Amer.*, vol. 59, Oct. 1969, pp. 1314-1321.
- [212] J. Stratton et al., *Spheroidal Wave Functions*. Cambridge, Mass.: M.I.T. Press, 1956.
- [213] W. Swindell, "A noncoherent optical analog image processor," *Appl. Opt.*, vol. 9, Nov. 1970, pp. 2459-2469.
- [214] C. W. Swonger and F. Y. Chao, "Computing techniques for correction of blurred objects in photographs," *op. cit.* [13].
- [215] M. Tasto and P. Wintz, "Adaptive block quantization," Dep. Elec. Eng., Purdue Univ., Lafayette, Ind., Rep. TR-EE 70-14, July 1970.
- [216] G. Toraldo di Francia, "Degrees of freedom of an image," *J. Opt. Soc. Amer.*, vol. 59, July 1969, pp. 799-804.
- [217] J. T. Tou, "Engineering principles of pattern recognition," in *Advances in Information Systems Science*, vol. 1, J. T. Tou, Ed. New York: Plenum, 1969.
- [218] S. Treitel and J. L. Shanks, "The design of multistage separable planar filters," presented at the Arden House Workshop on Digital Filtering, Harriman, N. Y., Jan. 1970; also in *IEEE Trans. Geosci. Electron.*, vol. GE-9, Jan. 1971, pp. 10-27.
- [219] O. J. Tretiak, "Approximating a matrix by a sum of products," *MIT/RLE Quart. Progr. Rep.* 98, July 1970.
- [220] O. J. Tretiak, E. Eden, and W. Simon, "Internal structure from X-ray images," in *Proc. 8th ICMBE* (Chicago, Ill., July 1969).
- [221] J. Tsujinchi, "Corrections of optical images by compensation of aberrations and by spatial frequency filtering," in *Progress in Optics*, vol. 2, E. Wold, Ed. Amsterdam, The Netherlands: North-Holland, 1963.
- [222] A. Vander Lugt, "Signal detection by complex spatial filtering," *IEEE Trans. Inform. Theory*, vol. IT-10, Apr. 1964, pp. 139-145.
- [223] S. Watanabe, "Feature compression," *op. cit.* [23].
- [224] C. S. Weaver, S. D. Ramsy, J. W. K. Goodman, and A. M. Rosie, "The optical convolution of time functions," *Appl. Opt.*, vol. 9, July 1970, pp. 1672-1682.
- [225] L. Weinberg, "Approximation and stability-test procedures suitable for digital filters," presented at the Arden House Workshop on Digital Filtering, Harriman, N. Y., Jan. 1970.
- [226] L. C. Wilkins and P. A. Wintz, "Bibliography on data compression, picture properties, and picture coding," *IEEE Trans. Inform. Theory*, vol. IT-17, Mar. 1971, pp. 180-197.
- [227] R. N. Wolfe, E. W. Marchand, and J. J. DePalma, "Determination of the MTF of photographic emulsions from physical measurements," *J. Opt. Soc. Amer.*, vol. 58, Sept. 1969, pp. 1245-1256.
- [228] H. Wolter, in *Progress in Optics*, vol. 1, E. Wolf, Ed. Amsterdam, The Netherlands: North-Holland, 1961, pp. 156-210.
- [229] J. W. Woods and T. S. Huang, "Picture bandwidth compression by linear transformation and block quantization," presented at the M.I.T. Symp. Picture Bandwidth Compression, Cambridge, Mass., Apr. 1969; also to appear in *op. cit.* [7].
- [230] E. C. Yeadon, R. A. Jones, and J. T. Kelly, "Confidence limits for individual modulation transfer function measurements based upon the phase transfer function," *Photogr. Sci. Eng.*, vol. 14, Mar.-Apr. 1970, pp. 153-156.



(a)

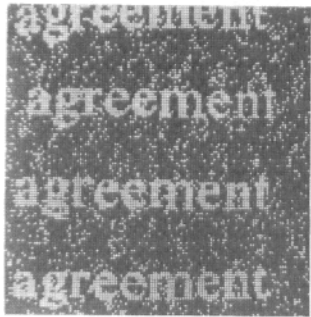


(b)



(c)

Fig. 3. (a) Original scene, digitized to 256×256 samples, with 256 brightness levels per sample. (b) Degraded image, obtained from the original scene by smearing (16-point average) in the horizontal direction. (c) Estimated impulse response of the degrading system. The intensity of the display is proportional to the magnitude of the impulse response.



(a)



(b)

Fig. 5. Nonlinear noise reduction. (a) Noisy image. (b) Noise reduced.



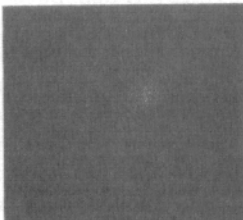
(a)



(b)



(c)



(d)



(e)



(f)

Fig. 6. Image crispening. (a) Original image $f(x, y)$. (b) $\sqrt{f(x, y)}$. (c) Magnitude of the Fourier transform of $\sqrt{f(x, y)}$. (d) Magnitude of the Fourier transform of \sqrt{f} multiplied by the frequency response of a high-pass filter. (e) $\sqrt{f(x, y)}$ high-passed. (f) Square of the high-passed \sqrt{f} .



(a)



(b)



(c)

Fig. 10. Images uniformly quantized to various numbers of levels (256×256 samples per frame). (a) 2 bits or 4 levels. (b) 3 bits or 8 levels. (c) 5 bits or 32 levels.



(a)



(b)



(c)

Fig. 11. Image logarithmically quantized to various numbers of levels (256×256 samples per frame). (a) 2 bits or 4 levels. (b) 3 bits or 8 levels. (c) 5 bits or 32 levels.



(a)



(b)



(c)



(d)



(e)

Fig. 12. The contour coding scheme of Schreiber and Graham. (a) Original (256×256 samples, 6 bits/sample). (b) Low-frequency part of the picture. (c) Synthetic highs. (d) Reconstruction (0.5 bit/sample).



{a}



{b}



{c}

Fig. 13. Hadamard block quantization (block size = 8×8).
Average number of bits per sample. (a) 1. (b) 2. (c) 3.



{a}



{b}



{c}

Fig. 14. Hadamard block quantization (block size = 16×16).
Average number of bits per sample. (a) 1. (b) 2. (c) 3.



{a}

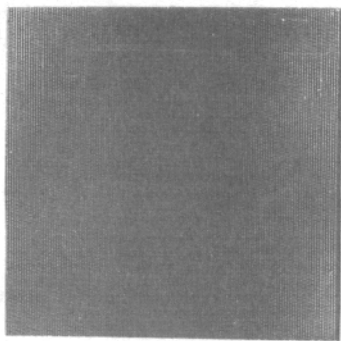


{b}

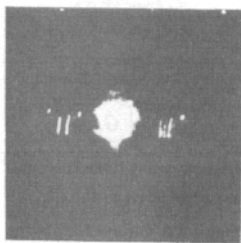


{c}

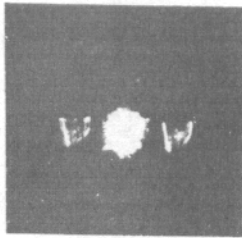
Fig. 15. Hadamard block quantization (block size = 1×256).
Average number of bits per sample. (a) 1. (b) 2. (c) 3.



(a)

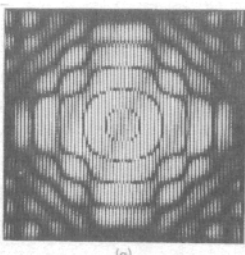


(b)

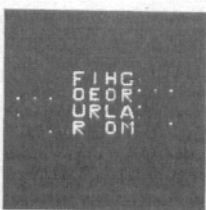


(c)

Fig. 16. Differentiation using a Lee filter. (a) Derivative filter. (b) Output pattern obtained using the letter "T" as input pattern. (c) Output pattern obtained using a sector of a circular disk as the input pattern.

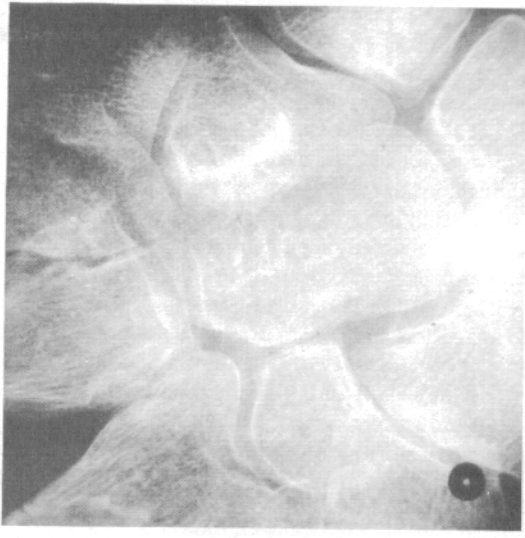


(a)



(b)

Fig. 17. Matched filtering using a Lee filter. (a) Matched filter for the letter "O." (b) Output pattern. Note that the input pattern appears in the center, while the desired output is at the periphery.



(a)



(b)

Fig. 18. X-ray picture. (a) Original. (b) High-pass filtered.

One then has access to nine points on the input image simultaneously and can operate on them electrically in parallel. In particular, we can take a weighted sum of the points to approximate linear filtering. Of course, for a good approximation, we need more points, i.e., a larger array of channeltron electron multipliers.